ABSTRACT

DEMETER, ASHLEY SAMANTHA. Performance Model and Assessment for VERAShift Beltline Fluence Calculations. (Under the direction of David J. Kropaczek).

While computers are built to be state of the art, the codes used by the nuclear industry have yet to catch up. Made to handle the known quantities of interest at the time, these programs are not adept enough to handle the pressing issues currently facing the industry. One such issue, neutron fluence, is of interest for plant lifetime and safety analysis. Neutron fluence is defined as the time integral of the neutron flux, typically in units of neutrons per centimeter squared. Accuracy on this value has wide implications for radiation shielding applications ranging from design to safety.

The Virtual Environment for Reactor Applications Core Simulator (VERA) is a new reactor physics suite of programs capable of detailed fuel rod power resolution (i.e. pin-by-pin) in the core that is comprised of the coupled deterministic transport code MPACT and the thermal-hydraulic subchannel code CTF. VERA can be coupled to the Monte Carlo code Shift for vessel fluence calculations via the core source terms. This coupling of codes referred to as VERAShift aims to create a high-fidelity program that is user-friendly in calculating vessel fluence.

The purpose of this research is to investigate the worthiness of this new code in terms of computational performance and accuracy. A motivating factor is the high computational resource required for VERAShift, which was designed to run on high performance computing platforms, and its applicability to run on industry-class machines. The end goal is to produce a reliable model that can accurately predict the behavior of the quantities of interest (QOI) for vessel fluence with respect to model input parameters, such as geometric fidelity, source resolution, and number of Monte Carlo particle histories. The two quantities of interest decided upon to be

measurements of the performance of the code were the Monte Carlo calculation time and relative error. Specifically, this research examines the effects of several factors to the VERAShift input on the vessel fluence calculation. By having a working model that accurately predicts the behavior of the VERAShift code, industry users will be able to determine if their current computer hardware can accomplish a fluence calculation within a certain time limit or to a certain degree of accuracy. Knowing this information up front will add value to the code as a viable option for beltline vessel fluence calculations worthy of replacing current legacy codes.

A realistic operating pressurized water reactor model was developed within VERAShift and the quantities of interest broken down into two separate investigations – time, then accuracy. The analysis of results for both series of test cases was performed the same. The method of Design of Experiments was used to first develop screening designs to identify the parameters of interest having the highest impact on performance and accuracy. This was then followed by development of a detailed model based on a reduced parameter set. From the information gathered and the model form selected, multi-linear regression was used to form a mathematical model of the output. Blind testing of the final model form indicates the model predicts the QOIs for the current VERAShift implementation.

Performance Model and Assessment for VERAShift Beltline Fluence Calculations

by
Ashley Samantha Demeter

A thesis submitted to the Graduate Faculty of
North Carolina State University
in partial fulfillment of the
requirements for the degree of
Master of Science

Nuclear Engineering

Raleigh, North Carolina

2018

APPROVED BY:

_____   _____
David J. Kropaczek   Scott P. Palmtag
Committee Chair

_____
Thomas W. Reiland

DEDICATION

For Mom & Dad.
It's always all been for you.

BIOGRAPHY

Ashley Demeter was raised outside of Cleveland, Ohio. She enjoyed science from a young age and began taking AP science classes while in high school. She attended Baldwin Wallace University in Berea, Ohio and obtained a bachelor's degree in physics. After inspiration from a senior year class, she decided to switch majors for graduate school and entered the field of nuclear engineering. She came to North Carolina State University in 2016 to begin her master's degree. Her research, under the direction of Dr. Dave Kropaczek and with funding from Oak Ridge National Laboratory, focused on code testing for VERAShift.

Outside of school, Ashley enjoys cooking and crafting. She likes trying new recipes and creating décor for around the house. She enjoys traveling home to see her friends and family in Ohio and spending time with her husband John.

ACKNOWLEDGMENTS

To her husband John, her family, and her friends, the author would like to extend her greatest appreciation for the unwavering support and extreme patience. Without them, none of this would have been possible.

The author would like to express her appreciation to her advisor, Dr. Dave Kropaczek, for the patience, guidance, advice, and honest discussion throughout this thesis. In addition to her advisor, the author would like to thank all those who provided insight and knowledge at North Carolina State University.

The author would like to express her appreciation to Dr. Tara Pandya, Andrew Godfrey, and the staff at Oak Ridge National Laboratory in Oak Ridge, TN, for the technical support that made this research possible.

TABLE OF CONTENTS

LIST OF FIGURES

LIST OF TABLES

ACRONYMS, DEFINITIONS, AND ABBREVIATIONS

2D	2 – Dimensional
3D	3 – Dimensional
BOL	Beginning of Life
BWR	Boiling Water Reactor
CADIS	Consistent Adjoint Driven Importance Sampling
CASL	Consortium for Advanced Simulation of Light Water Reactors
CDF	Cumulative Density Function
CE	Continuous Energy
CTF	COBRA-TF, Coolant Boiling in Rod Arrays – Two Fluid
DOE	Design of Experiments
DTK	Data Transfer Kit
ENDF	Evaluated Nuclear Data File
GG	Exnihilo General Geometry
HZP	Hot Zero Power
LWR	Light Water Reactor
MC	Monte Carlo
MeV	Mega electronvolt
MG	Multigroup
MPACT	Michigan Parallel Characteristics based Transport code
NRC	United States Nuclear Regulatory Commission
OFAT	One Factor at a Time
ORNL	Oak Ridge National Laboratory
QOI	Quantity of Interest
RPV	Reactor Pressure Vessel
RSD	Relative Standard Deviation
RTK	Reactor Tool Kit
SCALE	Standardized Computer Analyses for Licensing Evaluation
Shift	Hybrid Monte Carlo/deterministic radiation transport code
VERAShift	Coupled VERA and Shift codes
VERA	Virtual Environment for Reactor Applications Core Simulator
WBN1	Watts Bar Nuclear 1 Power Plant

1. INTRODUCTION

1.1 Overview

Neutron fluence is defined as the time integral of the neutron flux, typically in units of neutrons per centimeter squared. Accuracy on this value has wide implications for radiation shielding applications. Exposure from neutron radiation, particularly fast neutrons, causes damage and deterioration to the pressure vessel and other internal components of a nuclear reactor. The resulting embrittlement of the vessel and the welds reduces the lifetime of the vessel. The vessel is an irreplaceable component of a reactor; therefore, embrittlement and damage to structural integrity are pertinent issues in reactor safety and design.

Currently, the NRC requires a fluence calculation as part of its licensing procedures. There exists an NRC regulatory guide detailing the process of determining the best estimate of the fast neutron fluence, though it does not limit a company from using any particular means to accomplish this[5]. Several resources can be used in determining the vessel fluence, such as measurements or reactor physics codes that simulate neutron propagation.

One of these programs is the VERAShift package, a reactor physics code suite currently being developed by CASL, led by Oak Ridge National Laboratory. The VERAShift package couples VERA core simulator to the Monte Carlo code Shift to perform excore calculations in the vessel or other user specified locations based off a precise and detailed core and ex-core model.

Shift is "a new Monte Carlo (MC) radiation transport code developed for flexible, fast, and accurate transport solutions in a wide variety of application areas"[1]. For purposes of vessel fluence, Shift solves a fixed source problem with the sources provided by VERA. To accelerate the performance, Shift uses novel computer programing algorithms to identify weight windows

for the Monte Carlo vessel fluence calculation. The process uses the consistent adjoint driven importance sampling (CADIS) method, an automated variance reduction technique that removes the need for user intervention between iterations while also speeding up computational times as much as 1000 times[8]. This is achieved by biasing neutron particle histories towards regions of interest in the fluence calculation. VERAShift provides seamless integration allowing for execution of only one command and one input. The simple ASCII format of this input makes the program easier to interpret than some of its competitors, while it also decreases the intimidation that can be caused by the cryptic nature of some codes.

Together, VERA and Shift offer an improvement to the current state-of-the-art models. VERA produces high fidelity pin-by-pin power distributions, especially for peripheral fuel rods in regions of large power gradients. These pins represent the greatest influence on the fluence, and accurate pin powers imply more accurate vessel fluence calculations. Shift offers improved speed and performance fueled by the CADIS method. The coupled ability of the two programs to seamlessly feed information from VERA to Shift, then utilize this information for vessel fluence calculations reduces user intervention in the process reducing error. The easy interface aids in this goal and should require less training and time to learn before adoption by industry.

This report will discuss viability of the process, and not the verification, validation, or benchmarking of the programs. Benchmarking for Shift can be found in reference 1, and benchmarking for VERA can be found in references 2 and 3. Within the program are a plethora of options for geometric and material detailing, as well as for what output to produce. The resulting fluence from Shift will be dependent upon the inputs chosen. This report details the tradeoffs between detail, efficiency, and accuracy and what inputs offer the greatest yield for a given set of resources. Additionally, several input options for the code are explored to observe

their effects on the output. Performance of the current release of the code in terms of Monte Carlo run time and the accuracy of the fluence calculated is modeled such that industry may easily determine the input values and resources needed for code execution.

1.2 Current Industry Standards

Neutron fluence is defined as the time integral of the neutron flux, typically in units of neutrons per centimeter squared. Accuracy on this value has wide implications for radiation shielding applications. Exposure from neutron radiation, particularly fast neutrons, causes progressive damage and deterioration to the pressure vessel and other internal components of a nuclear reactor. The resulting embrittlement of the vessel and the welds reduces vessel lifetime. The vessel is an irreplaceable component of a reactor; therefore, embrittlement and damage to structural integrity are pertinent issues in reactor safety and design. Though pivotal to safe operation, determination of pressure vessel fluence has been historically difficult to predict, with many competing techniques existing. Precision of the neutron fluence outside of the reactor core is imperative for studies in safety and material effects.

The NRC's current regulatory guide for this calculation is Regulatory Guide 1.190 *Calculational and Dosimetry Methods for Determining Pressure Vessel Neutron Fluence,* which details accepted processes for determining the best estimate of the fast neutron fluence[5]. Several methods can be used in determining the vessel fluence, such as measurements or reactor physics codes that simulate neutron propagation. A company must determine the best estimate of the fast fluence for neutrons about 1 MeV by using computational methods with comparison to measurement when available. The geometry, material information, and neutron source must be explicitly defined with explanation of the propagation of neutrons to the vessel and uncertainty quantification and validation of the computational method used.

The NRC does not limit a company on what type of calculational methods to use for propagation of neutrons. Any type of deterministic method or Monte Carlo method are deemed acceptable under NRC Guide 1.190; however, the best estimate of the fluence at the beltline must be reported along with any associated uncertainties[5]. While deterministic codes give definite answers to the problem supplied, they can still be off due to suppositions that must be made for the code. Monte Carlo techniques have the advantage of precise geometry descriptions and continuous energy cross sections but are inhibitive due to their large computational cost. To reduce this burden, variance reduction techniques can be implemented such as neutron energy cutoff, source biasing, geometry splitting with Russian Roulette, and weight windows.

The main purpose of Guide 1.190 is to ensure that the fluence calculated for a light water reactor (LWR) is accurate enough to be used in determining the fracture toughness of the vessel to ensure that it will not fail. Guide 1.190 is used to determine the beltline fluence to be applied to the guidelines of 10 CFR 50, "Domestic Licensing of Production and Utilization Facilities" – specifically Appendix G, "Fracture Toughness Requirements" in addition to 10 CFR 50.61, "Fracture Toughness Requirements for Protection Against Pressurized Thermal Shock Events"[5]. NRC Guide 1.190 ensures both are satisfied by requiring the fast fluence of energies above 1 MeV with an overall uncertainty of 20% or less when calculating values for embrittlement and toughness, as defined in Appendix G and 10 CFR 50[5]. The guide also makes some suggestions for assumptions and methods deemed acceptable by the NRC.

The qualification of uncertainty occurs over three parts: "(1) the analytic uncertainty analysis (Regulatory Position 1.4.1), (2) the comparison with benchmarks and operating reactor measurements (Regulatory Position 1.4.2), and (3) the estimate of uncertainty in the calculated fluence (Regulatory Position 1.4.3)"[5]. The first part consists of checking the methodology for

accuracy. Uncertainty analysis must be performed on items such as nuclear data, geometries, isotopics, neutron sources, and any errors induced through methodology. These errors are combined statistically or algebraically to get the total calculational uncertainty or bias. For benchmarking, the fluence should account for any measurement uncertainties that may lead to differences in the calculated values. Simulator measurements from experiments by national labs or benchmark problems provided by the NRC can be used for methods qualification as well[5]. The third source of uncertainty comes from the calculation method, like the inherent uncertainty that arises when using a Monte Carlo method. The overall fluence calculation uncertainty is the combination of all three of these components and must remain below 20%. This research looks only at the third component of the overall uncertainty. Using NRC licensing standards, the target uncertainty for this research of this portion of the overall uncertainty was less than 5%.

1.3 Current Industry Codes

Current codes used for vessel fluence calculations consist of a mixture of discrete ordinates and/or Monte Carlo codes, which must be manually coupled to a core simulator code that provides the pin-by-pin power distribution, or equivalently source terms, for the fluence calculation. PARCS and SIMULATE are examples of current core simulator codes[15]. Deterministic codes currently used in industry rely on the nodal method for solving the multigroup diffusion or low order transport equations – done by splitting the core into a number of large regions called *nodes* and solving for over the entire node region. Pin power reconstruction is used to synthesize the pin-by-pin power distribution and is based on the use of homogeneous nodal solution and heterogeneous (2D lattice physics) solutions. Note that 2D lattice physics solutions, like those generated using CASMO, are used to generate cross section tables as a function of thermal-hydraulic conditions for the nodal method[35]. Both SIMULATE

and PARCS can perform eigenvalue, transient, xenon transient, decay heat, depletion, and adjoint calculations[15]. However, such codes cannot be used for extension beyond the core because of the diffusion approximation and the highly anisotropic scattering due to structural material and moderator beyond the physical core boundary.

It is noted that VERA is based on a deterministic transport solution (MPACT) coupled with thermal-hydraulic feedback at the subchannel level (CTF). In contrast to nodal methods, VERA solves for the power directly at the pin-by-pin level without the need for cross section homogenization and functionalization. In the end, both VERA and industry nodal methods provide the source terms used by the discrete ordinates or Monte Carlo code for the vessel fluence calculation.

Monte Carlo codes can provide more precise geometry representation of the vessel and ex-core components, but due to its being a statistical method, it will yield some error in the result, no matter how precise the geometry. The combination of codes and tradeoff of advantages and disadvantages is part of the issue when producing vessel fluence calculations. MCNP® and KENO are examples of Monte Carlo codes that allow for continuous energy neutron transport within a flexible geometry specification[15].

1.4 VERAShift

A new capability is VERAShift, a coupled reactor physics and ex-core code suite, currently being developed by CASL, which aims to greatly reduce the time and error associated with vessel fluence calculations. The VERAShift packages couples the VERA core simulator to the Monte Carlo code Shift to perform excore calculations in the vessel or other user specified locations based off a precise and detailed core model.

1.4.1 Shift

Shift is "a new Monte Carlo (MC) radiation transport code developed for flexible, fast, and accurate transport solutions in a wide variety of application areas"[1]. Shift employs a hybrid method, as discussed in the NRC regulatory guide, for biasing the neutron transport that is based on performing an adjoint calculation prior to the Monte Carlo vessel fluence calculation. The CADIS method is based on S_N discrete ordinates which is used to calculate Monte Carlo weight windows as a variance reduction tool to speed up the calculation time.

Shift uses a multitude of tallying interfaces including particles being born, streaming in a material, occurring collisions, fission, or being killed[1]. Shift uses "history-based statistics (as opposed to batch statistics) to determine the accuracy of the tally estimators" with the mean and variance outputed[1]. Path length tallies, performed over a volume, are used for cell or mesh tallies in Shift. These types of tallies are useful in estimating the flux in void regions, as well as in regions with small cross sections or regions where the number of collisions is unresolved[33].

$$\phi\,(x,E,t) = \, vN(x,E,t) \tag{1}$$

$$Where\ \phi\ is\ the\ flux\ \{cm^{-2}\sec^{-1}\}$$
$$N(x,E,t)\ is\ the\ number\ density$$
$$v\ is\ the\ velocity$$

The track length tally can be derived from the formula of the scalar flux, which can be interpreted as the total path length traveled per unit time per unit phase space by all particles[33]. Equation (1) can be rewritten to express this mathematically[33]

$$\phi\left(\vec{\xi}\right)d\xi = Rate\ at\ which\ particles\ generate\ path\ length\ in\ d\xi\ about\ \vec{\xi} \tag{2}$$

Integrating equation (3) over a phase volume gives[33]

$$\int_{\mathcal{R}}\phi\left(\vec{\xi}\right)d\xi = Total\ path\ length\ generated\ by\ particles\ in\ phase\ volume\ \mathcal{R} \tag{3}$$

By dividing by the volume and applying the mean value theorem, equation (2) can then be written as[33]

$$\bar{\phi} = \frac{1}{V} \int_{\mathcal{R}} \phi\left(\vec{\xi}\right) d\xi = \frac{Total\ path\ length\ generated\ by\ particles\ in\ \mathcal{R}}{V} \qquad (4)$$

In a Monte Carlo simulation, the right-hand side of this equation is found by scoring the total distance traveled by particles in a tally region, multiplied by the weight of the particle when applicable, and dividing by the tally region volume[33]. This is written formally, per particle history, by[33]

$$\hat{\phi} = \frac{1}{NV} \sum_{i=1}^{N} \sum_{c=1}^{C_i} w_{i,c} d_{i,c,\mathcal{R}} = \begin{cases} Total\ path\ length\ generated\ by\ particles\ in\ \mathcal{R} \\ per\ particle\ history \end{cases} \qquad (5)$$

$Where\ \phi\ is\ the\ flux\ \{cm^{-2}sec^{-1}\}$
$\quad d_{i,c,\mathcal{R}}\ is\ the\ distance\ travled\ by\ particle\ i\ in\ phase\ volume\ \mathcal{R}\ as\ it$
$\quad passes\ between\ events\ c-1\ and\ c.$

By default, Russian roulette is used for variance reduction. Shift also employs spatially and energy-dependent weight windows that can be directly implemented through an adjoint Denovo solution as an importance map[1]. By applying a normalization factor, the weight windows become "consistent" with the biased source created in Shift, thus employing the CADIS method. The CADIS method dramatically improves the speed and efficiency of the code. More on CADIS is discussed in the following section.

Shift uses a biased source to ensure "full consistency given a set of weight windows and a source definition"[1]. A space- and energy-dependent cumulative density function (CDF) is created to sample the mesh cells and energy groups and reject anything outside the source region[1]. An

estimated response is calculated using the following equation and the weight windows and renormalized accordingly[1].

$$R = \iint q(\boldsymbol{r}, E)\phi^\dagger(\boldsymbol{r}, E)\mathrm{d}E\mathrm{d}V = \iint \frac{q(\boldsymbol{r}, E)}{w(\boldsymbol{r}, E)}\mathrm{d}E\mathrm{d}V \qquad (6)$$

For hybrid calculations, Shift geometries are traced onto a cartesian mesh for use within Denovo. An approximate deterministic problem is solved, the fluxes are communicated back to Shift, then mapped onto the Shift mesh decomposition[1]. Currently, the code is written such that the entire barrel and vessel is tallied. For this research, CADIS mode is used and will be the only method described here on. The capabilities of CADIS mode can be seen in **Table 1**.

VERA calculates the power distribution in the core, then transfers the information to Shift to perform excore tallies. The information from VERA is transferred by memory and is not written to a file. The code allows for parallel execution of multiple state points and tallies to be conducted in user defined areas. Shift and VERA each use their own sets of processors, which allows for them to do state point calculations concurrently. The number of processors is a combination of those required for VERA in addition to the number requested for the decomposition of the adjoint deterministic calculation in CADIS mode which is described below. Using the general geometry features of Shift allows for excore details of the core barrel and vessel as well as other features outside of the barrel, including detectors or plant specific details to be employed with greater ease than previous codes. The information from VERA is passed seamlessly to Shift through the VERA common input which helps to reduce errors associated with having different models for different codes.

Figure 1 below shows a simplified flow for VERAShift. First, a global communicator between VERA and Shift is established, though each program runs on its own set of processors independent of the other[2]. The VERA calculation is the performed and the Data Transfer Kit

(DTK) is set up to transfer data from VERA to Shift[2]. The VERA calculation is performed for a state point then transfers the information to Shift. Shift then launches a state point calculation. Since they use different processors, VERA will then continue to the next state point, when applicable, while Shift runs the previous one. VERA must finish a state point before Shift can begin that state point though. For the Shift calculation, first an adjoint calculation is done followed by the MC calculation. Shift runs the requested number of particles and outputs the vessel flux tally in an HDF5 file. Information is passed at the end of each MPACT state point and passed to Shift, updating it for the next state point's calculation. The simulation is complete once both MPACT and Shift finish all state points.

The following quantities can be passed from VERA to Shift:

- "in-core fission source from MPACT eigenvalue calculation;

- Isotopics for pincells and inserts using the short list of tracked nuclides: ^{234}U, ^{235}U, ^{236}U, ^{238}U, ^{16}O, ^{135}Xe, and ^{10}B;

- Boron concentration in coolant;

- Temperatures in fuel, clad, coolant of pincells and inserts; and

- Density of coolant in pincells and inserts."[2]

Additional details on the theory and methodology of Shift independently and its use in VERA can be found in references 1 and 2.

```
 1: Parse VERA-CS input
 2: Set up MPI communicators
 3: Construct VERA-CS and Shift model evaluators
 4: Set up MPACT-to-Shift and CTF-to-Shift transfers
 5: for each state do
 6:     if processor running VERA-CS then
 7:         Run a coupled VERA-CS single statepoint calculation or a predictor-corrector depletion
    calculation
 8:         Send isotopics, temperatures, densities, fission source, and stop criteria
 9:         Continue to next state
10:     else if processor running Shift then
11:         Receive isotopics, temperatures, densities, fission source, and stop criteria
12:         while !stop criteria do
13:             Run Shift forward or CADIS calculation and tally flux in vessel
14:         end while
15:     end if
16: end for
```

Figure 1: Algorithm showing simplified VERAShift simulation flow [2].

1.4.2 CADIS

All variance reduction techniques aim to increase the number of particles contributing to a certain quantity or entering a certain location. This can become complicated in 3D modeling and often needs to be performed iteratively to develop proper variance reduction parameters[8]. Variance reduction can help to reduce the overall time needed for a calculation, but often is specific to the problem of interest, and new parameters must be changed when the problem type or quantity of interest changes. Further comments on previous techniques used to combat this issue can be found in reference 8.

One variance reduction technique built into Shift is the *consistent adjoint driven importance sampling* technique (CADIS)[8]. CADIS uses the P_N adjoint function to perform

11

automatic variance reduction by using weight windows to bias both the source and transport of

neutrons[8].

Table 1: Capabilities of Shift for CADIS mode [1].

Capability	CADIS
Energy	MG and CE
Geometry^a	meshed RTK for SP$_N$ adjoint and GG for MC
Particles	n or n-γ
Isotopics	depleted isotopics in fuel, control rods, inserts, and boron concentration via VERA-CS
Temperature	fuel, cladding, and moderator temperatures via VERA-CS
Parallelism	domain replicated
Tallies	cylindrical mesh (vessel) flux with energy bins (through VERA input); user-defined tally definitions enabled through supplemental input (see [8])
Source	SP$_N$ adjoint source is uniform energy detector response in vessel; MC source is same as Forward

CADIS is not only an automated variance reduction technique, but it also offers weight

window parameters in both energy and space and a consistent biased source distribution[14]. It can

be applied to transport problems involving estimates of scalar quantities and is used for

accelerating single tallies. An initial deterministic calculation is performed for the adjoint,

followed by a calculation of the weight windows which are inversely proportionate to the adjoint

scalar flux. The space- and energy-dependent weight windows, shown in equation (7), is

determined from the estimated response R and the adjoint flux, ϕ^+. The consistent biased source,

$\hat{q}$, as shown in equation (8), is determined from the response, the adjoint flux, and the original

source q. The use of a consistently biased source distribution ensures that "source particles are

preferentially sampled in regions of high importance"[14].

$$w = \frac{R}{\phi^+} \qquad\qquad (7)$$

$$\hat{q} = \frac{q \, \phi^+}{R} \qquad\qquad (8)$$

The CADIS technique offers the benefit of being automatic – it requires no user intervention between iterations of calculating weight windows. In practice, defining weight windows requires detailed knowledge of the space- and energy-dependence of areas of the core. Consequently, this can be difficult to achieve and requires much adjusting between iterations to ensure particles are being directed in directions that are important. The use of CADIS as a biasing technique helps to drastically improve the computational performance of a code. Since this technique is already built into the VERAShift framework, it requires only the activation of a command within the VERA input to utilize. The CADIS technique used in Shift requires little experience with biasing nor does it require previous experience of preceding runs. The reduction of user intervention, effort, and time when crafting weight windows helps to make VERAShift a more reliable code for large scale reactor applications.

1.4.3 VERAShift

Together, VERA and Shift offer an improvement to the current state of the art models. VERA produces high fidelity pin-by-pin power distributions especially for the peripheral pins that are subject to large neutron flux gradients due to leakage. These pins represent the greatest influence on the fluence, and accurate pin powers imply more accurate vessel fluence calculations. Shift offers improved speed and performance fueled by the CADIS method. The coupled ability of the two programs to seamlessly feed information from MPACT to Shift, then utilize this information for vessel fluence calculations, reduces user intervention, and in the process, reducing error. The

easy interface aids in this goal and should require less training and time to learn before implementing into industry. The simple input can reduce a model from hundreds of thousands of lines typical for a complicated MCNP® model, to a few hundred lines for the coupled depletion and Monte Carlo codes.

Initial verification for the vessel fluence and excore detector calculations has been completed, helping to ensure that the VERAShift code is compliant with NRC Guide 1.190. Exact transfers of isotopics, fuel temperatures, information on cladding and moderator, in addition to the fission source previous described, provide a very detailed neutron source as required by Regulatory Guide 1.190. The exactness of the VERA power distribution can lead to high memory requirements though and this is part of the investigation within the VERAShift performance model. In addition to each constituent code, the verification of the excore components of VERAShift are vital in proving the worth and accuracy of the methods used in the program suite. To do this verification, full core Watts Bar like models were analyzed for expected behavior of the fission source between state points in addition to looking at the importance map generated by Shift for expected trends[32]. In addition to this, 15 cycles of Watts Bar Unit 1 were used for verification of the capabilities. The calculated maximum fluence for these results agreed with back calculated fluence reference values[32]. Full details of the verification thus far of VERAShift can be found in reference 32.

By all intents, VERAShift could qualify as contender for use in industry. It follows much of the NRC regulatory guide with ample benchmarking, verification and validation of both results and methodology. Within the VERAShift program suite lies an abundant amount of resources for a company that make the determination of vessel fluence simple – so long as the company has the resources to run such codes. Without the need for user intervention between

codes, overall error is reduced, as there is no loss of geometric detail or other sort of information miscommunication. VERA calculates the neutron source, transfers it to Shift, which then propagates neutrons to the vessel, where tallies are performed so that vessel fluence can be determined. VERAShift provides a method to determine a best estimate fluence that requires a simpler input, which is hugely beneficial to the field, but the feasible use of the code in industry remains to be determined. **Table 2** below demonstrates the advantages of VERA compared to the common industry standards. Greater details on VERA can be found in Reference 3.

Table 2: VERA Capabilities for Reactor Core Simulations (italics represents items under development) [3].

Capability	VERA-CS	Typical Industry Methods
Neutron Transport	3D (2D/1D) whole-core pin-resolved transport based on actual fuel, core, and support structure geometry	Transport-based 2D infinite lattice physics + 3D nodal diffusion theory with approximate reflectors
Cross Section Energies	Finer energy group structures (47 groups) but minimized for performance	Lattice physics in hundreds of groups with 3D diffusion in few groups (2-3)
Pin-by-pin Powers	Explicit 3D pin and intra-pin powers on fine axial mesh	3D pin average powers reconstructed from 2D infinite lattice calculations and nodal solution
Thermal-Hydraulics	Directly coupled multi-phase sub-channel for each flow channel (between fuel rods) with cross flow	Simplified single-phase lumped channel models for nodal neutronics with detailed sub-channel bounding analyses uncoupled
Fuel Mechanics	*Directly coupled for intra-pin fuel temperature feedback and cladding stress calculations.*	Simplified average fuel temperature models for nodal neutronics with detailed risk analyses uncoupled
Instrumentation	Direct in-core *and ex-core* instrument response models	In-core response from 2D infinite lattice calculations; no ex-core models
Short Lived Fission Product Poisons	Explicit pin-by-pin buildup, decay, and depletion of Xenon and all fission products via detailed decay chains	Average Xenon and Samarium concentrations tracked nodally without feedback to pin powers
Depletion	Explicit intra-pin depletion at actual local spectral conditions, *including component depletion such as control rods and instrumentation*, and including explicit pin-by-pin shutdown decay calculations	Depletion performed explicitly at 2D lattice levels for various anticipated spectral and geometric conditions and pin exposures inferred at 3D level from node-average exposure for approximate spectral conditions
Spacer Grids	Direct effects on neutron flux, depletion, instrument response, and T/H	Typically not explicitly resolved or included in neutronics calculations
CRUD	Direct accumulation of CRUD containing boron based on sub-channel steaming, with feedback to neutrons and depletion	CRUD not modelled directly but assessed for risk as a post-processing step to the analyses.
Safety Analysis	Direct calculations for parameters such as DNB, PCI, CFM, etc	Bounding analyses performed separate from neutronics, sometimes with manual iteration between physics
Gamma Transport	*3D gamma transport for local energy deposition and instrumentation response*	Gamma transport in 2D at the lattice physics level and included only in the relative pin power distributions
Neutron Fluence	*Direct accumulation in structural components for lifetime evaluations*	Approximated from few group nodal flux in nearest fuel locations
Computer Resources	Single statepoint calculations in ~30 minutes on ~4000 cores, in quarter symmetry	Neutronics single statepoint calculations in < 1 minute on 1 core following a few hours to pre-tabulate cross sections. Detailed T/H and fuel mechanics calculated separately.

2. METHODOLOGY

VERA is a suite of coupled multiphysics packages that can easily model LWR reactor cores with high fidelity. The main components of VERA are MPACT (neutronics) and CTF (thermal-hydraulics). VERAShift ties together the VERA core model capabilities and Shift (Monte Carlo) for ex-core calculations. The VERA Common Input file contains all the information needed to run VERAShift options requested by the user. It compresses the need for multiple codes and inputs into a single, simple ASCII file input which contains the information for all aspects of the model.

VERA offers pin-resolved transport for explicit power descriptions on a finely resolved axial mesh with multi-phase and sub-channel flow between rods. The VERA specific input allows for modeling in-core instrumentation, like control rods and space grids, to be easy and simple. Buildup, decay, Xenon, and Boron concentrations can be tracked accurately. The geometry capabilities within VERA provide options based on the accuracy necessary and computational resources available. By having a greater understanding of these tradeoffs, appropriate inputs can be chosen for desired modeling.

Shift builds off these capabilities by creating a fluence and ex-core capability within VERA. Using detailed isotopics as well as well-defined pin powers to calculate vessel fluence should make for more accurate best estimate values. The hybrid MC method takes advantage of variance reduction techniques which greatly reduce the time needed to perform the vessel fluence calculation, where traditionally this is a computationally exhaustive method. VERAShift works by running Shift as a fixed source problem in forward or CADIS calculation mode to produce vessel fluence results. The following section details the communication between the

components of VERA, Shift, and inputs when running VERAShift for vessel fluence calculations.

2.1 Scope of Research

Much of the information set forth by Regulatory Guide 1.190 remain outside of the scope of this thesis. Details such as justification for cross sections, unit testing for VERAShift, benchmarking, verification and validation can be found in other documents such as those in references 1-3 and references 9-12.

This research aims to develop a systematic and efficient approach in which to determine VERAShift input parameters of highest influence on the output QOIs. Two main QOIs will be investigated: the amount of time the program takes to finish the Monte Carlo calculation and a measure of accuracy of the fluence calculation. The research will focus on calculating fluence at the *beltline* region of the fuel for neutrons between 1 MeV and 20 MeV, as required for validity for NRC. For this research, the beltline region will hence forth refer to the portion of the RPV that is adjacent to the active fuel region, a common definition in industry for this term[20].

The QOI for amount of time was quantified as the amount of time necessary to complete the Monte Carlo calculation within Shift. The total simulation consists of three time components – the VERA calculation, the MC Shift time (which includes the adjoint calculational time), and the amount of time for data transfers, setting up geometries, loading cross section data, and all other internal communications – referred to here as "other" time. As will be shown, this other time remains fairly constant throughout the VERAShift calculation, regardless of any problem definition.

Since all Monte Carlo calculations inherently have uncertainty, it is important to be able to properly analyze the associated errors. The relative standard deviation (RSD) was chosen as

the QOI for quantifying the accuracy of a solution. The RSD measures the amount of dispersion

of a distribution and is defined by taking the standard deviation and dividing it by the mean, as

seen in equation (9). The mean flux is the average flux within a defined tally region within the

vessel with its associated variance. The standard deviation is the square root of this associated

variance. The RSD is useful in expressing the precision and repeatability of the value. By

modeling this value, a company looking to get a certain accuracy of their answer would be able

$$\sigma_{rel} = \frac{\sqrt{\sigma^2}}{\varphi} \tag{9}$$

Where σ_{rel} is the relative standard deviation
σ^2 is the variance
φ is the mean flux

to quickly identify the necessary parameters and ultimately end up with an amount of time

necessary to run the code.

This research also gives insight into the current implementation of the code. For instance,

the source definition will affect the accuracy. By having different source resolutions in the form

of varying axial discretizations of the VERA model, insight can be gained on how the refinement

of the source affects the outputted absolute fluence in addition to the relative standard deviation.

By observing the effects of the number of source regions used, the possibility of using a

simplified source while still obtaining accurate fluence values is entertained.

Another input parameter of interest is the order of the Legendre polynomial used in the

adjoint calculation and its effect on the accuracy of the output QOIs. Accounting for higher order

angular flux moments should produce more accurate source biasing and weight windows that, in

turn, should result in more accurate flux values and lower relative standard deviations for a given

number of Monte Carlo particle histories. More accurate weight window will reduce the number

of histories needed to run, and will therefore, also reduce the run time of the code.

The method of design of experiments is used to reduce the number of inputs that were deemed most crucial to the output via a screening design. This then allowed a thorough examination of these selected inputs for an overall performance assessment of the VERAShift code with respect to the Monte Carlo execution time and accuracy. Collected data from several runs of varied inputs then allows for construction of a mathematical model. Once put forth, this model is used to predict the output behavior of the code and to test the validity of the model itself.

2.2 Model Characteristics

The input used is a modified version of CASL Progression Problem 5. The Progression Problems within CASL are a series of increasingly more complicated modeled situation designed by industry members within CASL as a framework for development. The input used is referred to as problem 5A-2D, a 2D slice of a Watts Bar Nuclear 1 (WBN1) Power Plant like nuclear core. The problem was also modified to be a 3D, henceforth referred to as 5A-3D, model having a total height of 366.71 cm and an active fuel height of 365.71 cm. Details such as inserts and spacer grids are excluded from the input to keep the input simple, however these could be easily added. Additionally, although Shift can transfer many things from VERA to the Monte Carlo calculation, only the fission source was transferred due to memory limitations. Problem 5A-3D is a quarter core model of "a complete quarter core loading of Westinghouse 17x17-type fuel assemblies arranged in the WBN1 initial loading pattern. The fuel is at beginning-of-life (BOL) and Hot Zero Power (HZP) isothermal conditions"[2]. The model used was ran for only a single state point calculation and did not include a depletion calculation. The conclusions of the performance model developed are easily extrapolated from a state point to a full multi-cycle analysis as fluence is effectively an accumulation of single state point edits (i.e. flux multiplied

by time). **Figure 2** below demonstrates the layout of the enrichments of the fuel rods in addition to the placement of control rods in quarter symmetry.

	H	G	F	E	D	C	B	A
8	2.1	2.6 20	2.1	2.6 20	2.1	2.6 20	2.1	3.1 12
9	2.6 20	2.1	2.6 24	2.1	2.6 20	2.1	3.1 24	3.1
10	2.1	2.6 24	2.1	2.6 20	2.1	2.6 16	2.1	3.1 8
11	2.6 20	2.1	2.6 20	2.1	2.6 20	2.1	3.1 16	3.1
12	2.1	2.6 20	2.1	2.6 20	2.6	2.6 24	3.1	
13	2.6 20	2.1	2.6 16	2.1	2.6 24	3.1 12	3.1	
14	2.1	3.1 24	2.1	3.1 16	3.1	3.1		
15	3.1 12	3.1	3.1 8	3.1	Enrichment Number of Pyrex Rods			

	H	G	F	E	D	C	B	A
8	D				D			
9								
10								
11								
12	D				D			
13								
14								
15								
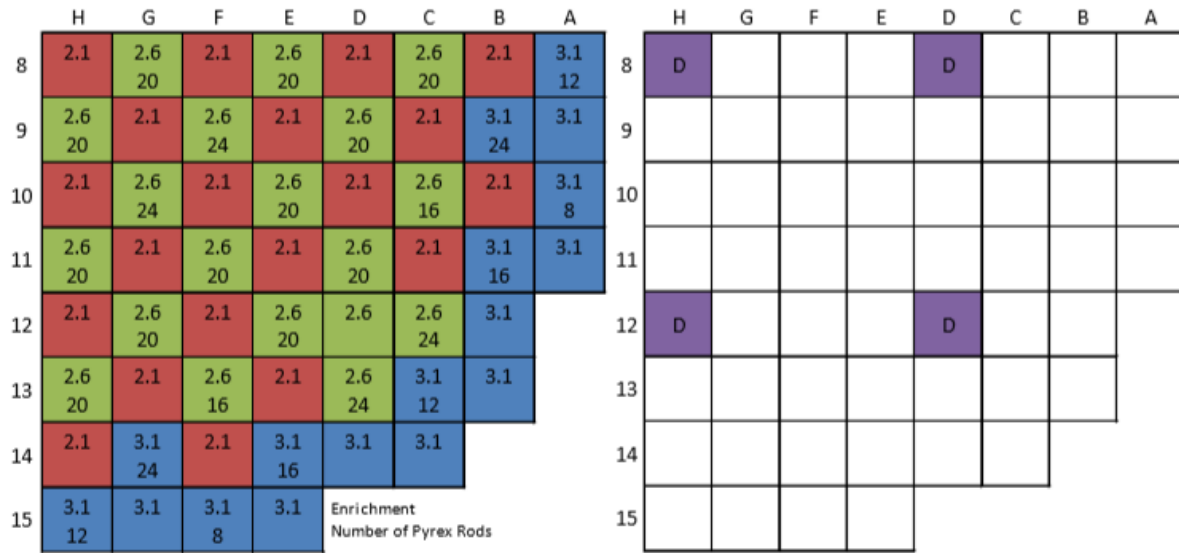
Figure 2: Problem 5a-2D Assembly, Poison, and Control Rod Layout (Quarter Symmetry) [2].

Within the VERA Common Input is the MPACT block and the Shift block. The majority of the changes to the input occur in these two places, with the exception of adding addition axial bounds to change the model from one node to several. All information in all blocks of the input apply the same in VERAShift as they would if only running VERA. Full information on all inputs to the Shift block for VERAShift can be found in Reference 2.

Geometric meshing takes place on three separate levels. The first occurs on the VERA side under the *axial_edit_bounds* of the VERA common input. This divides the active fuel region of the core into user defined regions. These values are used in the decomposition of space in the adjoint calculation of the deterministic solution at the beginning of the Shift calculation. The values are not explicitly the same, but the values of the axial levels in MPACT are used as a baseline for levels but are limited in size by inputs in the Shift block. These inputs adjust the parameters for the deterministic mesh which ensures that mesh edges exist at least at the edges of

the axial bounds in MPACT. These values are used for the adjoint calculations. Lastly are the tally mesh regions, also described within the Shift block. These values control the size and number of tally regions used for the axial, radial, and azimuthal directions. More information on the tally regions can be found in Section 3.2.

2.3 Model Parameter Input Cases

The inputs under CTF were not investigated under this research. Therefore, cases were ran with feedback from CTF turned off except for when unique pins were enabled to ensure proper transfer of the information. Feedback was turned off to help with reduce the overall runtime of the VERA calculation since the runtime of the MC calculation only was of interest. When unique pins are turned on in the Shift block, each pincell has a unique composition of isotopes, temperatures and densities passed from VERA. When disabled, Shift uses the initial material definitions in the VERA input to make compositions for all the pins and other objects. More details on inputs selected and changed for this research can be found in section 2.4.2. Full geometric and material descriptions for the input can be found in Reference 2. An example input can be found in Appendix 1.

The tally regions sizes were based off the deterministic mesh requirements in Guide 1.190. Both the tally region and deterministic mesh sizes were set to at least meet the requirements of the NRC for licensing. For the radially tally regions, a minimum of 1.5 tally regions per inch of steel in the vessel is required. The axial tally mesh needed is 0.5 tally regions per inch of fuel. The angular resolution requirement is a minimum of 40 tally regions per octant, or 80 regions per quarter core. The numbers picked for these designs range from 1 up to values greater than that required for the NRC licensing process. VERAView, a visualization tool developed at ORNL to work alongside VERA, was used to facilitate selection of cases for the

screening design which were differentiated by the number of tally regions. **Figure 3** displays a portion of the vessel at progressively increased resolutions with respect to the tally regions. As shown on a graduated color scale, the ring closest to the top represents the most refined tally region while the bottom represents the least refined tally region.

The cases were split up into a series of separate testing suites to determine a model for the Monte Carlo calculation time, the accuracy of the model, and a set used to test the final equations. All cases were run on institutional cluster called *Panacea* at ORNL. These input categories will be discussed below.

To test the performance of the code in terms of how quickly the Monte Carlo code works, a selection of inputs was determined that are suspected to have the most influence on the calculation time. These inputs were determined to be the number of particle histories, the number
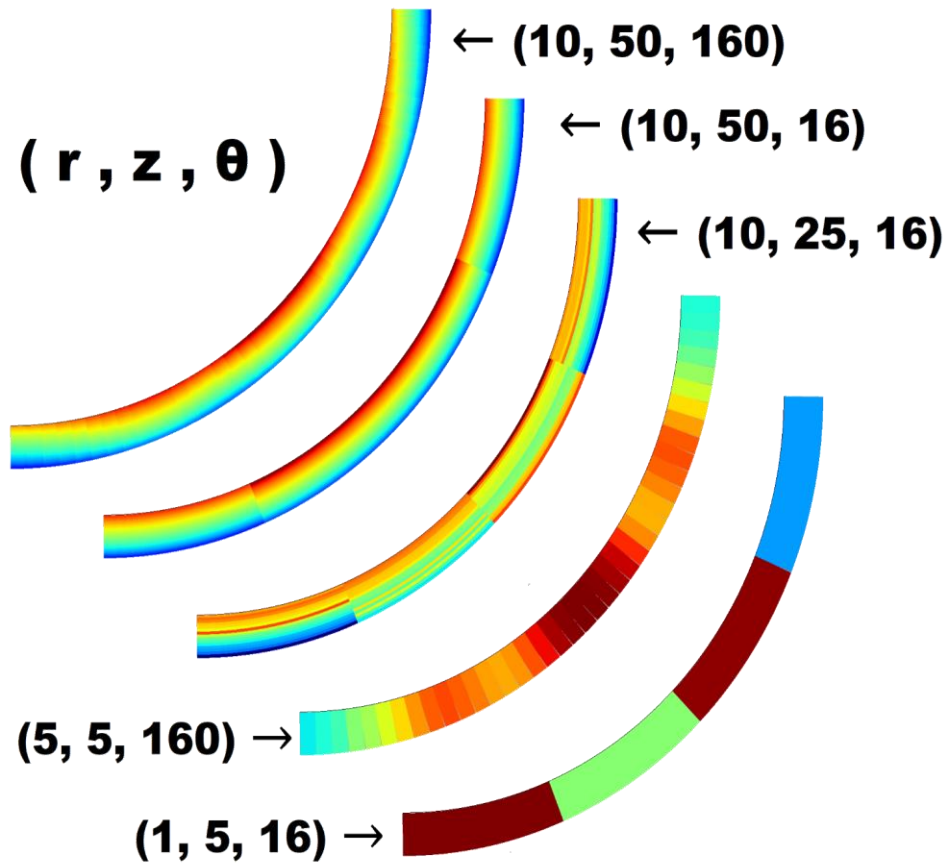
Figure 3: Visualization of different refinements of tally regions.

of cores used in the MC calculation, the number of tally regions, the number of source regions

(axial levels in MPACT), and whether unique pins were used for the calculation. The number of

tally regions includes the axial tally regions, azimuthal tally regions, and radial tally regions. As

a precursor to performing the screening design, a few test cases were run to determine if any one

tally region affected the run time or if it were the total number of tally regions that impacted the

time. **Table 3** and **Table 4** demonstrate the test cases performed to test this. Based off the small

differences in time, for the timing cases, only the number of total tally regions was varied, not

the individual components. More information on the selection of inputs can be found in section

2.4.2.

Table 3: Settings for the axial, radial, and azimuthal tally regions for the three test cases.

	Test 1	Test 2	Test 3
Axial	10	5	1
Radial	10	15	20
Azimuthal	12	16	60
Total	1200	1200	1200

Table 4: Values for the Shift calculation time for the three test cases and the associated differences between the values of each test case.

	time (sec)	%dif1	%dif2	%dif3
Test 1	283.93		1.78%	2.91%
Test 2	289.08	-1.81%		1.15%
Test 3	292.45	-3.00%	-1.17%	

For the accuracy test cases, a similar approach was taken. The inputs of interest chosen were determined to be the number of particle histories, the number of cores used in the MC calculation, the number of tally regions, the number of source regions (axial levels in VERA), and whether unique pins were used for the calculation. For this set of cases, the tally regions were not condensed, and instead kept as three separate variables: axial, azimuthal, and radial. More information on the selection of inputs can be found in section 2.4.2.

2.4 Construction of Mathematical Model of Code Performance

Using design of experiments, the seven inputs selected were tested to determine the critical few needed to model the QOIs. A screening design was used to quickly reduce the input parameter space. A full factorial design was used on the most important variables to further investigate their impact on the time and accuracy components. When only the crucial inputs remained, a final DOE was used to construct a mathematical model using input values that abide by the requirements of the NRC. The model build from these cases was then tested against a set of blind cases to test the validity and predictability of the output.

2.4.1 Design of Experiments

A Design of Experiments (DOE) is a very powerful scientific method of planning and conducting an experiment that yields the cause and effect relationships between variables. It is a structured way to change multiple settings to understand their impact on a process in an efficient and effective manner. So called "one-factor-at-a-time" (OFAT) experiments are one way to study the effects of a variable on an output, but is not an actual DOE process, nor is it efficient. Doing a single factor analysis like OFAT can often lead to missed combinations or interactions that would yield optimal solutions when tested. OFAT experiments are dangerous and ineffective methods since they do not test every combination of factors like a DOE does.

DOEs are most commonly used when more than one input is suspected of having influence on an output of interest. These types of experiments look at the overall interactions of a factor, which includes effects caused by the presence of one or more other factors. Interaction effects can be more important than single effects, and since interactions are not ignored, the results do not point to false conclusions. DOEs allow for a systematic investigation of these interactions in a more reliable and complete way compared to OFAT experiments.

There are many types of DOEs, such as screening experiments used to "screen" inputs for the most influential and worthy inputs that are worth further investigation. Full factorial DOEs test factors across all possible combinations to determine which are statistically significant, while optimization DOEs used to identify optimal factor settings to hit predetermined targets. Depending on the aim of the study and the resources available, different DOE models may be used. **Figure 4** shows the comparison between the robustness of a DOE design and the number of factors which a design can handle.
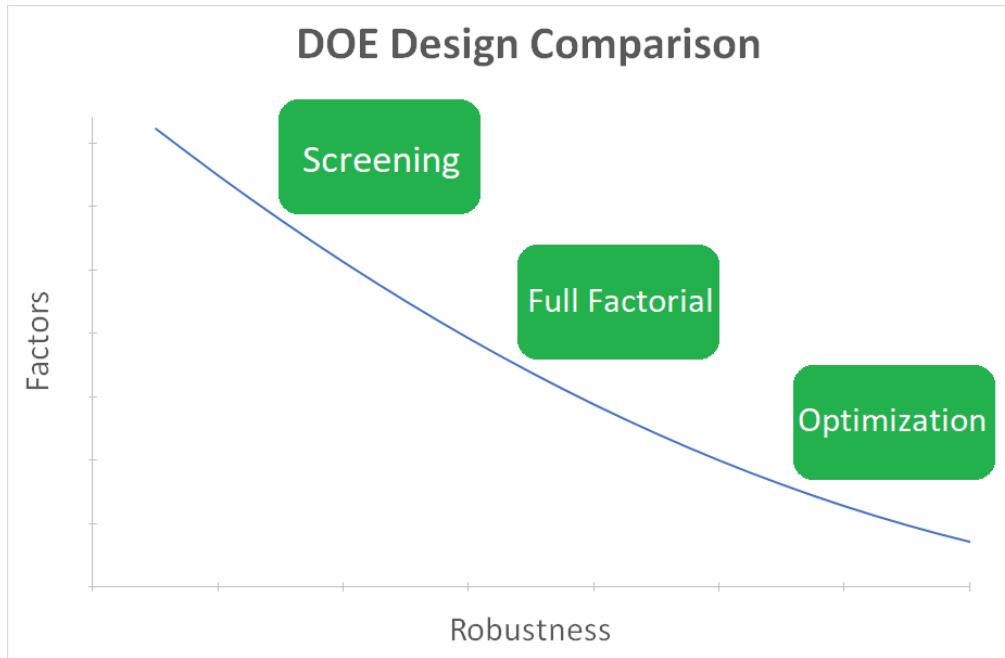
Figure 4: Chart demonstrating the flow of DOEs from screening designs through to optimization.

Regardless of the type of design to be used, a DOE can be broken down into several

steps. To begin, one must determine the objectives of the experiment, so forth referred to as the

outputs, as well as the input variables that will be studied, referred to as the *factors* or *inputs*. For

the design to be most effective, careful thought must go into picking factors. Factors that are

impactful should be chosen and noise factors – those that cannot be controlled – should be

avoided. To construct a DOE, the factors must be given levels which are allowable values for the

factor to be set at from which data on the output will be collected. More information on the

selection of inputs for this research can be found in section 2.4.2. Once inputs, outputs, and

levels are decided on, a number of test runs are calculated. Test runs occur at the given levels for

each of the factors in different combinations. These combinations yield full factorial or fractional

factorial designs with differing resolutions.

The number of runs necessary for a *full factorial* design can be found simply through

$$runs = LEVEL^{factor} \qquad\qquad (\,10\,)$$

27

Which describes all possible combinations of factors and levels[16]. For instance, an experiment with three factors and two levels (a high level and low level) for each factor would have a total of eight runs for a full factorial design. A large number of runs is characteristic of full factorial designs, but they test every combination of factor levels which yields the most complete information on interactions. More on full factorial designs can be found in section 2.4.4.

When the number of factors increases significantly, it may be impractical to do a full factorial design. To effectively handle a large number of factors, *screening* designs can be implemented in order to eliminate those factors which do not influence the output much. More on screening designs can be found in section 2.4.3. When the number of factors is larger but not significantly larger, a fractional factorial design can be used in place of a full factorial design. Fractional factorials use a subset of runs from a full factorial design and are used when a full set of runs is too costly or impractical based on resources[16]. Fractional factorials can lead to confounding of interactions, leading to less accurate modeling.

Confounding, also known as aliasing, occurs when a variable not being controlled in an experiment still has an effect on the output[16]. When using fractional factorial designs, some interactions can be missed due to using only a subset of runs and confounding occurs. This means that "the effect of the factor cannot be mathematically distinguished from the effect of another factor"[16]. To combat this issue, higher resolution designs can be used when creating the design matrix of runs.

The *resolution* of the fractional factorial designs must be considered. The resolution is a design's ability to "separate main effects and low-order interactions from one another"[17]. While most outputs are controlled by a few main effects, choosing higher resolution designs can

uncover lower order confounding. The most advantageous resolutions are III, IV, and V, as lower resolutions do not distinguish confounded effects and resolutions above V become similarly as costly as doing a full factorial design. **Figure 5** demonstrates the different resolutions and their respective abilities.

Resolution	Ability	Example
I	Not useful: an experiment of exactly one run only tests one level of a factor and hence can't even distinguish between the high and low levels of that factor	2^{1-1} with defining relation I = A
II	Not useful: main effects are confounded with other main effects	2^{2-1} with defining relation I = AB
III	Estimate main effects, but these may be confounded with two-factor interactions	2^{3-1} with defining relation I = ABC
IV	Estimate main effects unconfounded by two-factor interactions Estimate two-factor interaction effects, but these may be confounded with other two-factor interactions	2^{4-1} with defining relation I = ABCD
V	Estimate main effects unconfounded by three-factor (or less) interactions Estimate two-factor interaction effects unconfounded by two-factor interactions Estimate three-factor interaction effects, but these may be confounded with other two-factor interactions	2^{5-1} with defining relation I = ABCDE
VI	Estimate main effects unconfounded by four-factor (or less) interactions Estimate two-factor interaction effects unconfounded by three-factor (or less) interactions Estimate three-factor interaction effects, but these may be confounded with other three-factor interactions	2^{6-1} with defining relation I = ABCDEF

Figure 5: Chart showing different resolutions and their abilities for fractional factorial designs [17].

Once a design is chosen along with the factors and levels to be observed, the information is put into a matrix that describes the order of the runs and which levels to use for which factors. The design matrix systematically changes the input factors to optimize the information obtained using a predetermined number of runs[16]. These runs are conducted using the prescribed values and the data for the outputs is collected. Once all the runs are complete and the required data has been entered, the information can be analyzed, and the information obtained can be used to

optimize the values of the factors. More information on the analyzing and implementation of results can be found in section 3.

DOEs are effectual ways of identifying relationships between cause and effect and provide understanding of interactions among causative factors. These sorts of experiments can aid in optimizing the reliability of a results, minimizing the error of relationships, and maximizing learning using minimum resources by maximizing the amount of information gained from each experimental run. OFAT experiments can miss key relationships and interactions between factors and are wasteful of resources. DOEs are economical and help to build mathematical models based off interactions. DOEs can generate a model which explain the output by setting the factors to different values.

To construct and analyze the DOE experiment used for this research, Minitab 18 was used. Minitab is an industry leading code for looking at statistical data and is widely used and trusted by professionals to improve and optimize processes by simplifying the input of data, identifying trends and patterns, and extrapolating answers for given problems.

2.4.2 Selection of inputs

The common input for VERAShift allows for a multitude of inputs to be changed for MPACT, CTF, and Shift. The purpose of this research is to flesh out the most important of those inputs when observing the time to perform the vessel fluence calculation as well as the accuracy with which the result is produced. These two quantities were decided upon to be measurements of the performance of the code.

Inputs were selected by brainstorming a list of variables available to the VERAShift input and deciding on those which were believed to be the most influential while eliminating those that likely do not impact the output as much. **Table 5** lists the inputs selected for this study

and their respective levels used in the screening design. For completeness, all inputs were given three levels, except for unique pins, which can only be either on or off.

Table 5: Selected inputs and descriptions for the screening design cases.

	Low	Middle	High	Input Variable	Input Description
Particles	100,000,000	1,000,000,000	10,000,000,000	`Np`	Number of particles used in the Monte Carlo calculation
Shift Cores	100	225	400	`num_blocks_i` `num_blocks_j`	Number of cores used in the Monte Carlo calculation; separate from those used by MPACT/CTF
Shift Axial	1	5	10	`num_axial`	Number of axial tally regions for the vessel fluence binning
Shift Radial	5	25	50	`num_radial`	Number of radial tally regions for the vessel fluence binning
Shift Aximuthal	16	88	160	`num_theta`	Number of azimuthal tally regions for the vessel fluence binning
Unique Pins	off (-1)		on (+1)	`create_unique_pins`	Makes all pincell compositions unique
MPACT Axial	1	5	10	*requires several changes to input	Number of axial levels in the MPACT model; 2D versus 3D

Ideally, input levels should be considered somewhat extreme, but not entirely "off the scale." The should be far enough apart to accurately represent reality without being too close and missing some subset of possible or realistic values.

2.4.3 Screening Design Implementation

Full factorial DOEs can be computationally expensive and time consuming when the number of factors grows large. In the case of this research, seven input variables were selected to analyze and determine the effect on the output. To complete a full factorial of this design, over 1,000 runs would need to be conducted. To reduce this to a more feasible number of runs, a screening design was first conducted using two levels for each variable. Screening is very helpful in collecting base line data and taking an initial look at output performance.

Screening takes a relatively small number of runs of the given factors to perform a preliminary analysis to determine which factors are heavy contributors to the desired output. From there, a higher resolution design or full factorial can be ran based on the lessened number of factors determined to be the most influential to optimize the inputs. Screening designs reduce the number of runs required to do analysis, but this assumes that there are no interactions. Their purpose is to screen out factors that have little or no effect on the output. Screening is very efficient at eliminating unimportant factors but are simple to set up, analyze, and create a frame work for more complex designs.

Screening designs rely on a series of principles. First is the sparsity of effects which concludes the main inputs create the greatest impact on the output while 1st, 2nd, up to n^{th} order interactions decrease in importance as their order increases[19]. Aliasing, also known as confounding, relates to the resolution of the design and accounts for higher order interactions between factors with higher resolution of a design[19]. Screening designs mostly take place at Resolution III. The effect of the heredity principle states that "in order for an interaction to be significant, at least one of its parent's main effects should be significant"[19]. The principle is used to determine whether to keep certain factors when moving on from a screening design to a higher resolution design or full factorial design. More information on the screening designs used in this research can be found in sections 3.1.1 and 3.1.2.

2.4.4 Full Factorial Design Implementation

Of options available, full factorial DOE offers the best compromise between number of variables analyzed and robustness of the model. Full factorials keep from *aliasing* factors. In other words, factors will not be confounded, and each effect can be investigated individually, including higher order interactions.

These types of design use the full number of runs as shown in equation (10). The use of screening designs helps to reduce the number of important inputs, thus reducing the number of runs needed for the full factorial design. Once the screening design was analyzed and the number of factors reduced, a full factorial design was performed for the remaining variables of interest. More information on the full factorial designs used in this research can be found in sections 3.2.1 and 3.2.2.

3. RESULTS

Minitab was used for the analysis of the outputs of both the screening designs and full factorial designs. Minitab calculates statistical relationships between input variables and the outputs of interest. Many of these applications of Minitab will not be used for this research, however, the main applications of it for this research will be discussed below.

A regression analysis was performed to determine the relationship among variables and outputs and in predictive applications. To do this analysis, seven assumptions about linear regressions must be met. The first two require that both the independent and dependent variables, the inputs and outputs of interest, are continuous variables[29]. These two assumptions are fundamental to the current area of study and are not checked by Minitab. The remaining assumptions are principles that can be checked in Minitab through different plots and graphs. The third assumption requires a linear relationship between the inputs and outputs[29]. This can be checked in Minitab by producing a scatter plot of the output and inputs and visually checking for linearity. Fourth, there are to be no significant outliers in the data set[29]. Minitab has built in tools to help with identifying outliers in the data so as not to negatively affect the regression fit due to their presence. The fifth assumption is that the observations are independent of one another[29]. Homoscedasticity, the principle that variance along the line of best fit remains constant along the

line, is the sixth assumption[29]. Lastly, the residuals should have an approximate normal distribution[29].

To determine which inputs would be deemed important for a final performance model, a significance threshold was decided on for the inputs in question. This value is called the significance level, denoted by α, is found by taking 1 minus the confidence level of the analysis. For this research, the significance level used is 0.05 with a two-sided confidence level of 95%.

Part of the analysis of a DOE involves the analysis of variance. The Analysis Of Variance chart shows the p-value for all the linear terms in the model, which are then compared to the significance level α in addition to other statistics. An example of an analysis of variance table can be seen in **Figure 6**.

The p-value is a test against the null hypothesis. The null hypothesis argues that the model does not account for any of the variance in the response. This ties into the significance level, 0.05 for this research, meaning there is a 5% risk of assuming the model explains some variance when in reality it does not[28]. When the p-value is greater than the significance level, no conclusion can be reached about the explanation of variance in the model. When the p-value is below the significance level, it can be concluded that the model does account for the variance and represents stronger evidence against the null hypothesis[28]. Values of p that are less than that of α are therefore concluded as important to the model. As shown in **Figure 6**, parameters listed with p-values of highest significance include Particles, Cores and Axial discretization. Much of

this research relies on analyzing the p-value itself for statistical analysis of the importance of each input to the final performance model.

Analysis of Variance

Source	DF	Seq SS	Contribution	Adj SS	Adj MS	F-Value	P-Value
Model	18	1501459	96.69%	1501459	83414	12.97	0.000
Linear	6	1072553	69.07%	1072553	178759	27.80	0.000
Particles	2	739574	47.63%	739574	369787	57.50	0.000
Shift Cores	2	158669	10.22%	158669	79335	12.34	0.004
MPACT axial	2	174310	11.22%	174310	87155	13.55	0.003
2-Way Interactions	12	428906	27.62%	428906	35742	5.56	0.011
Particles*Shift Cores	4	212623	13.69%	212623	53156	8.27	0.006
Particles*MPACT axial	4	181022	11.66%	181022	45255	7.04	0.010
Shift Cores*MPACT axial	4	35261	2.27%	35261	8815	1.37	0.326
Error	8	51446	3.31%	51446	6431		
Total	26	1552905	100.00%				

Model Summary

S	R-sq	R-sq(adj)	PRESS	R-sq(pred)
80.1919	96.69%	89.23%	586001	62.26%

Coefficients

Term	Coef	SE Coef	95% CI	T-Value	P-Value	VIF
Constant	173.8	15.4	(138.2, 209.4)	11.26	0.000	
Particles						
10000000	-136.8	21.8	(-187.2, -86.5)	-6.27	0.000	1.33
100000000	-96.0	21.8	(-146.4, -45.7)	-4.40	0.002	1.33
Shift Cores						
100	106.7	21.8	(56.4, 157.0)	4.89	0.001	1.33
225	-36.8	21.8	(-87.2, 13.5)	-1.69	0.130	1.33
MPACT axial						
1	-113.6	21.8	(-163.9, -63.2)	-5.20	0.001	1.33
5	53.2	21.8	(2.8, 103.5)	2.44	0.041	1.33
Particles*Shift Cores						
10000000 100	-95.7	30.9	(-166.9, -24.6)	-3.10	0.015	1.78
10000000 225	34.0	30.9	(-37.2, 105.2)	1.10	0.303	1.78
100000000 100	-77.6	30.9	(-148.8, -6.4)	-2.51	0.036	1.78
100000000 225	20.9	30.9	(-50.2, 92.1)	0.68	0.517	1.78

Figure 6: Example chart showing the different outputted information from Minitab.

Modeling statistics are useful in determining the fit of the model to the data. The R^2 (R-sq) term represents what percent of the variance is explained by the model[23]. A higher R^2 term indicates that the model fits the data very well. In the example shown in **Figure 6**, the R^2 value is 94.42%, meaning that the model fits the data well. The adjusted R^2 value (R-sq (adj)) adjusts the R^2 relative to the number of inputs used[23].

Another way to analyze the screening design is to visually inspect the p-values. Two graphs of the outputs were generated: the pareto chart of standardized effects and the normal plot of standardized effects. In statistics, the effect is a measurement of the size of the variance explained by the model[30]. This differs from error, which explains how much is *not* explained by the model. The effect size quantitatively measures the magnitude of this effect. Standardized effects allow for comparison of effects across different models by removing the variables in the effect. Standardized effects are normalized to the standard deviation of the output. It is found by taking the difference of two means and dividing it by some combined value of the standard deviations[30]:

$$Standardized\ Effect = \frac{|\overline{x_1} - \overline{x_2}|}{\sigma_{pooled}} \tag{11}$$

$$\sigma_{pooled} = \sqrt{\frac{(n_1 - 1)s_1^2 + (n_2 - 1)s_2^2}{n_1 + n_2 - 2}} \tag{12}$$

$$s_1^2 = \frac{1}{n_1 - 1}\sum_{i=1}^{n_1}(x_{1,i} - \overline{x_1})^2 \tag{13}$$

Where: $\overline{x_1}$ is the mean

σ_{pooled} is the combined standard deviation for two independent data sets

n_1 is the size of the data set

s_1^2 is the variance for a group of data

3.1 Primary Screening Results

3.1.1 Analysis of Primary Screening Design for Time Output

This research aims to create a model for the time performance of the Monte Carlo calculation within VERAShift. A screening design was first created using the inputs of interest as defined in section 2.4.2. The screening design reduced the total number of inputs from seven to three. Determination of the important from unimportant variables was determined by visually inspecting the pareto chart and normal plot.

The pareto chart shows the absolute value of the standardized effects in decreasing order of value of importance. In addition to plotting the standardized effect, a reference line is shown that indicates which values are important. This line, determined by the significance level, shows which of the inputs are most important statistically. The pareto chart simply tells which are important in changing the output – it does not indicate the magnitude with which it affects the output. For the x-axis, the scale is calculated by "dividing each coefficient by its standard error (Coef/SE Coef)"[25]. The reference line represents the (1-α/2) quantile of the fitted normal distribution[25].

The normal plot shows the standardized effect against a normal distribution fit with a standard deviation of one[22]. The value and location of the inputs are important. Negative numbers indicated a decrease in the output and those values which are farthest away from zero have the greatest impact on the output[22].

When the p-values are greatly above the significance level, that input is removed from the analysis and deemed no longer significant statistically to the results. This assessment is performed using either the analysis of the variance chart or the visual graphs. The model is then

refit without the unnecessary inputs to reduce the model, the p-values are reevaluated, and this process continues until all p-values are less than the significance level.

As previously mentioned, the "other" time consisting mostly of data transfers and internal code communication was investigated for consistent behavior. Data taken from the test cases used from the time design of these experiments was looked at to determine if this time changed with the changing inputs. As can be seen in **Figure 7**, the time needed to perform these parts of the calculation remains consistent in a belt of time ranging from about 40 to 100 seconds, depending on whether or not unique pins was turned off or on respectively.
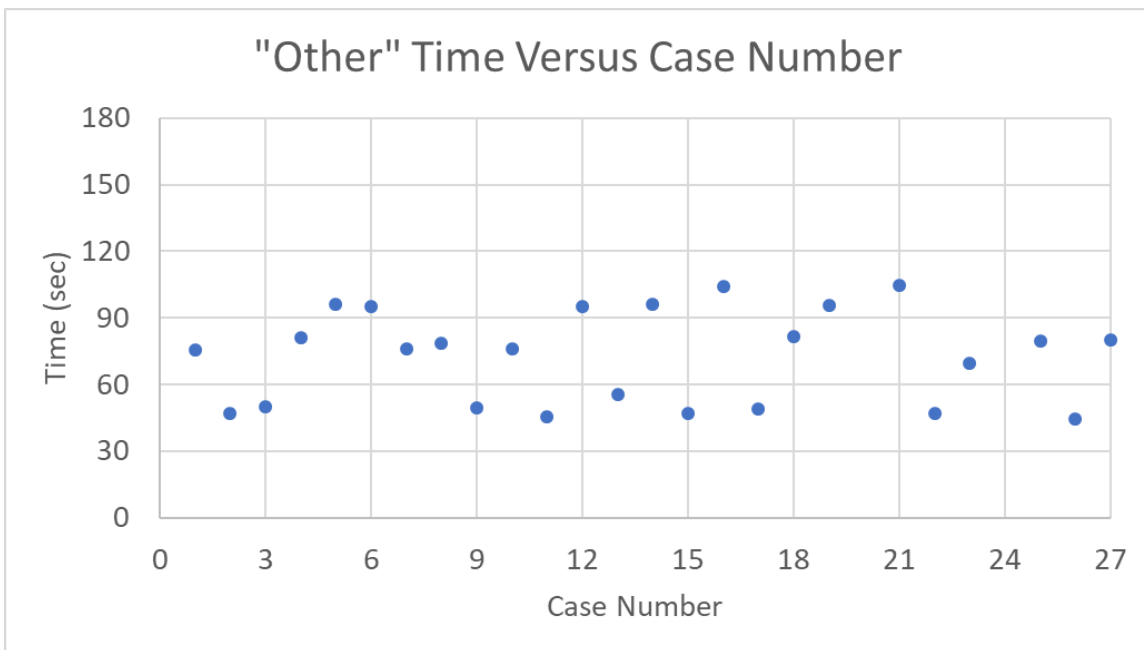
Figure 7: Graph demonstrating the time taken in seconds to complete the "other" portion of the calculations, based off the results from the timing study.

As seen in the first sets of graphs, **Figure 8** and **Figure 9**, all five inputs were looked at. The pareto chart shows that input C, the number of tally regions, has the least effect on run time. The normal plot echoes this result. To better generate a model, this input was removed, and the analysis reran in Minitab. This was done again after it was determined that input D, the use of unique pins, was also statistically unimportant.
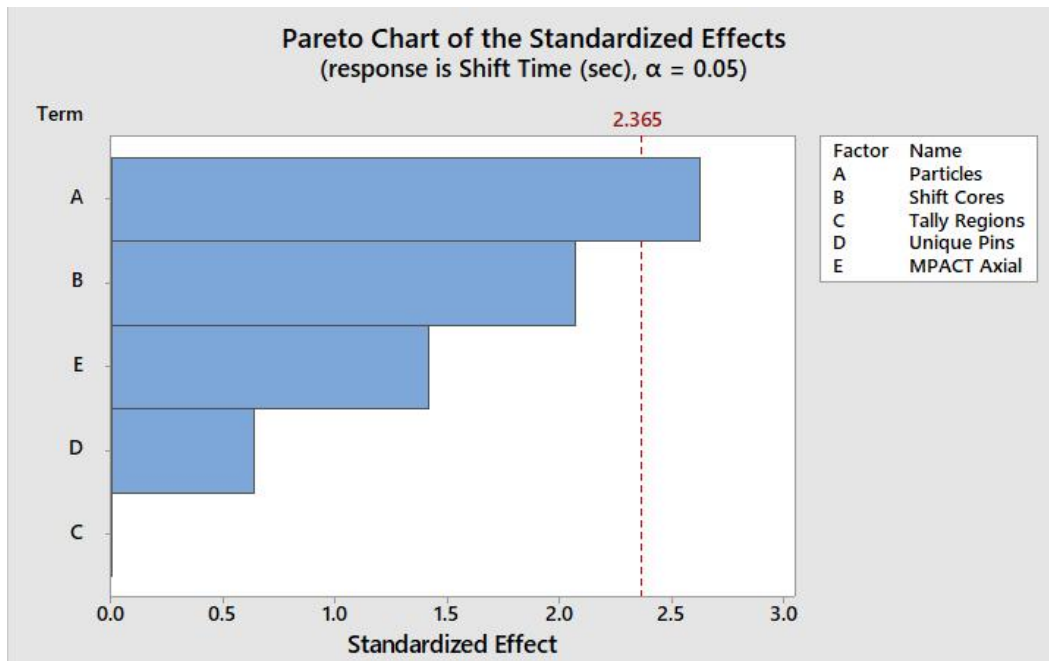
Figure 8: Pareto chart showing all five factors used in the screening design. The red line indicates the reference line for significant and insignificant inputs.

Figure 9: Normal Plot showing all five factors used in the screening design. The red line indicates the normal distribution used to compare the values of the inputs. Inputs farthest away from the distribution line are most influential to the output.

Figure 10 and **Figure 11** show both inputs A and B are statistically important. For this research, input E, the number of source regions for the MPACT calculation, was also kept for additional testing due to it being close to the reference line on the pareto chart and comparably far away from the distribution line on the normal plot. It was expected that the number of particles and the number of cores used in the calculation would be the two most influential parameters in the calculation time.
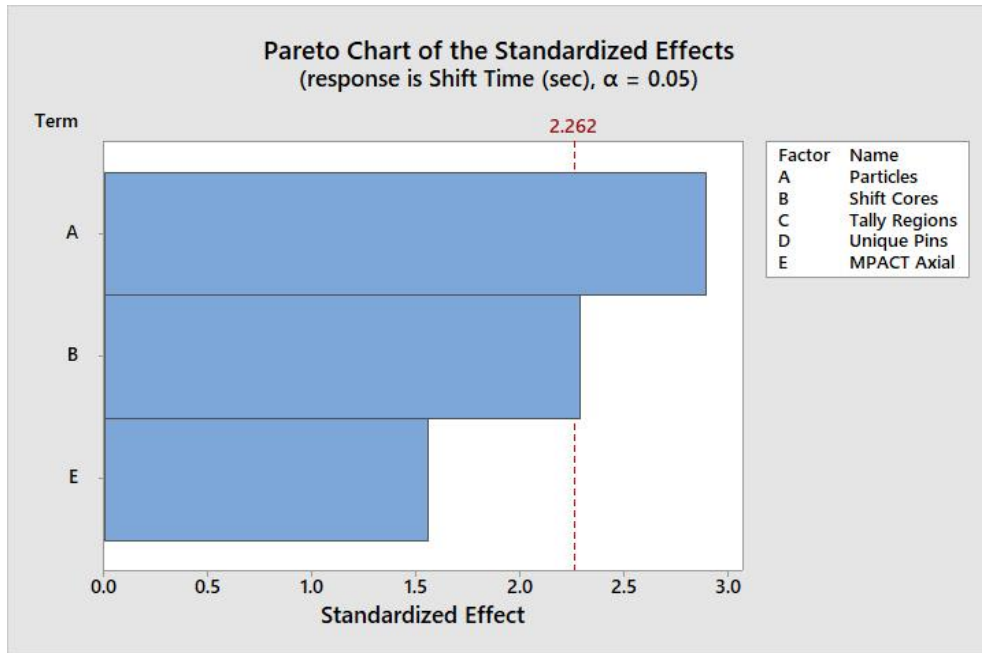
Figure 10: Pareto chart showing the three remaining factors.
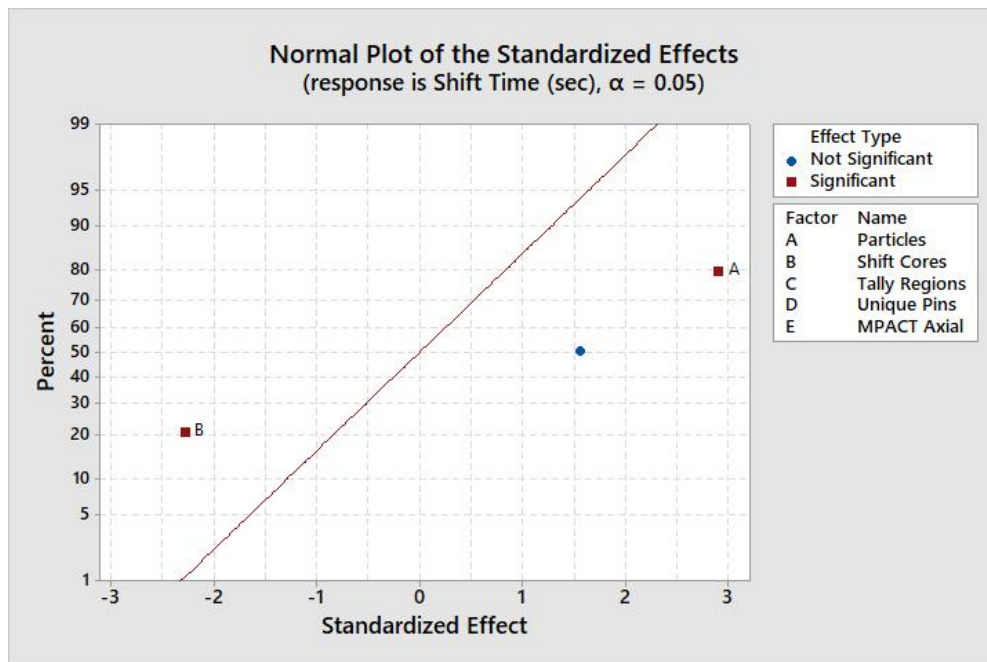
Figure 11: Normal plot showing the three remaining factors.

3.1.2 Analysis of Primary Screening Design for Accuracy Output

A total of seventeen runs were used to conduct the initial testing on the accuracy inputs. As with the time component, all seven inputs were initially looked at in the production of the pareto and normal plots in Minitab. Seen in **Figure 12** and **Figure 13** below, the least important inputs were removed from the analysis and the data reanalyzed. In total, four remaining inputs, which can be seen in **Figure 14** and **Figure 15** remained for further testing of the accuracy component.
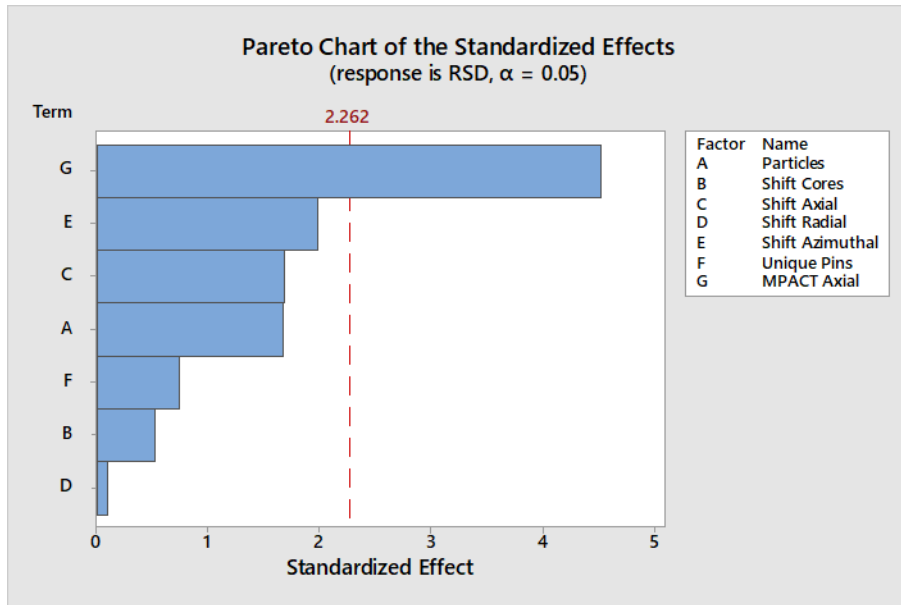
Figure 12: Pareto chart showing all seven factors used in the screening design. The red line indicates the reference line for significant and insignificant inputs.
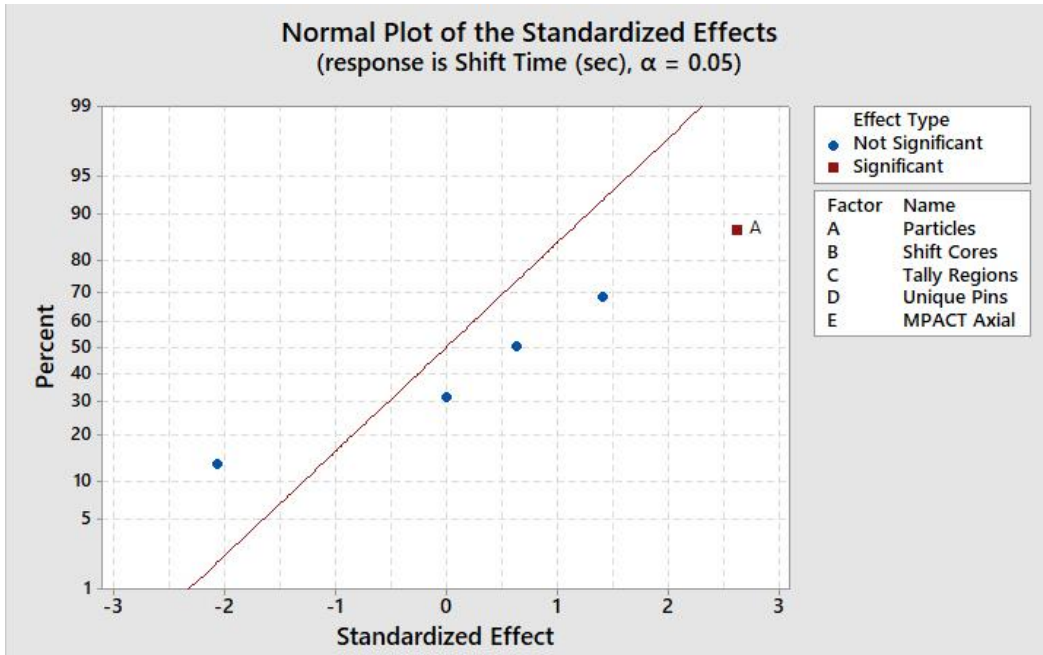

Figure 13: Normal Plot showing all seven factors used in the screening design. The red line indicates the normal distribution used to compare the values of the inputs. Inputs farthest away from the distribution line are most influential to the output.

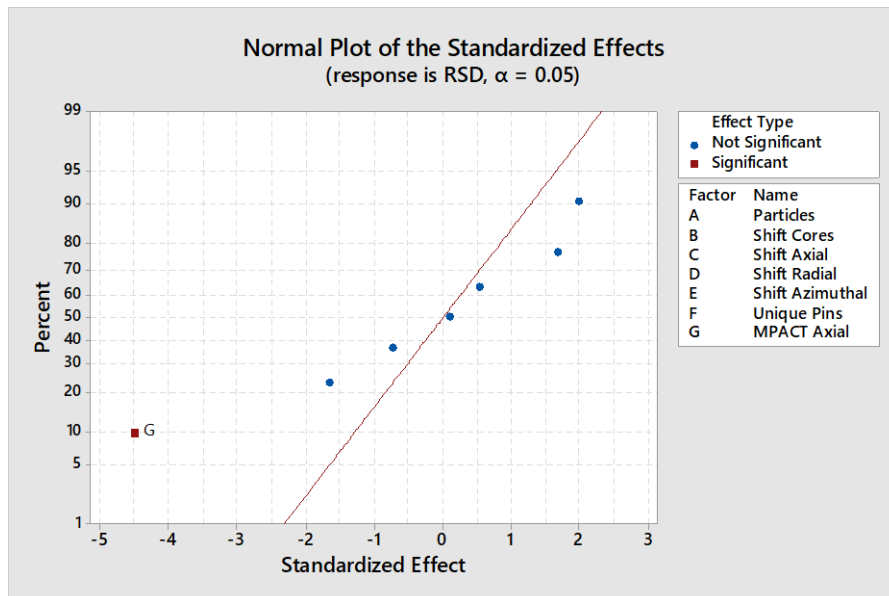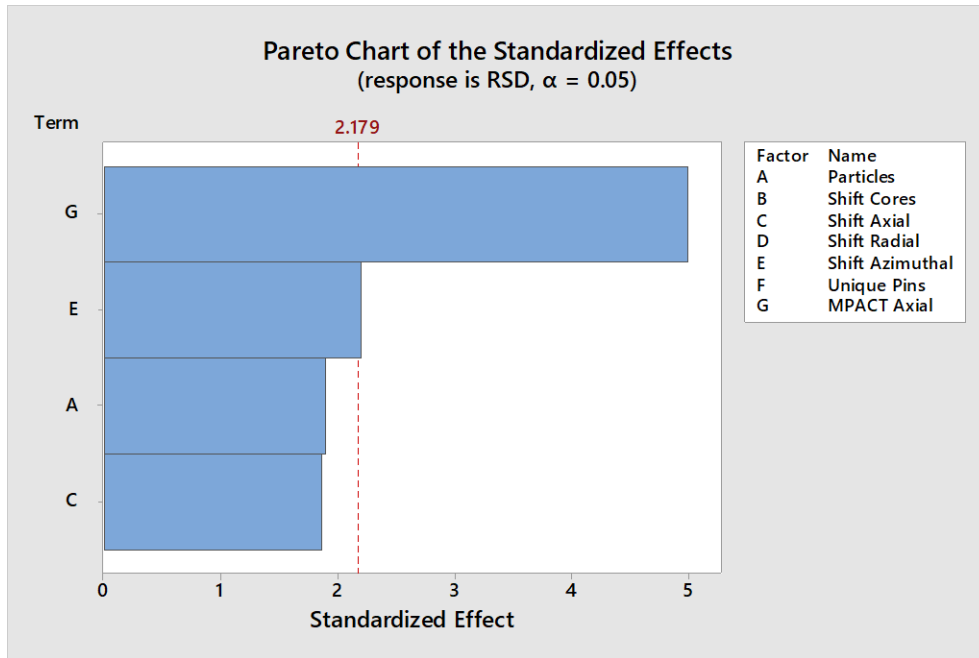**Figure 14: Pareto chart showing the four remaining factors.**
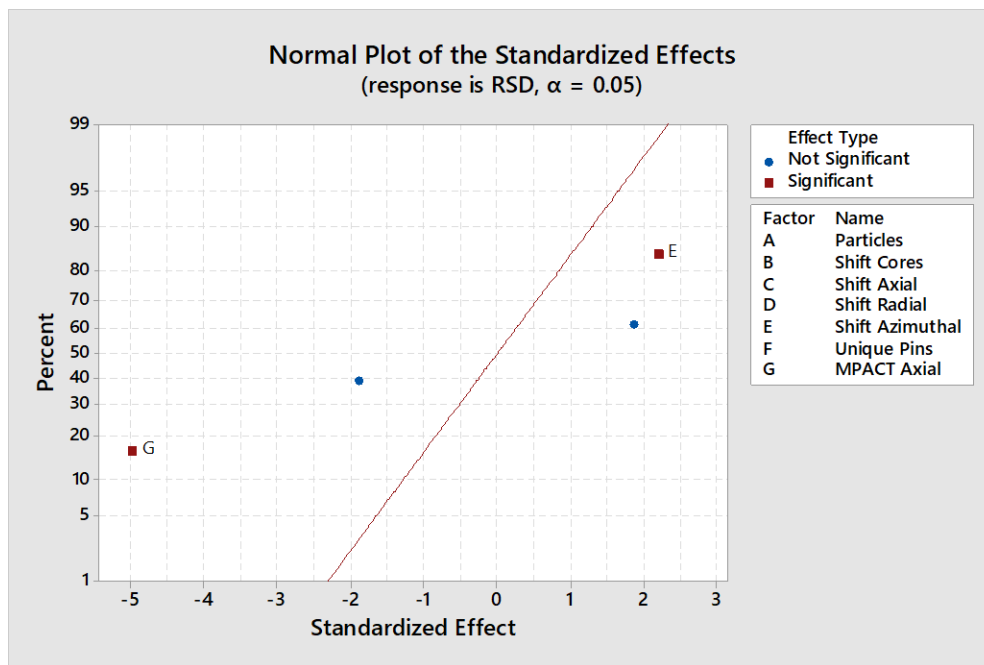
Figure 15: Normal plot showing the four remaining factors.

3.2 Full Factorial Design Results

A second round of testing was performed looking only at the three remaining variables for both the time and accuracy results. A full factorial design was used for these, for a total of twenty-seven runs and eighty-one runs for the time and accuracy cases respectively. For the full DOE analysis, the inputs levels were changed slightly for the model to be applied to a greater variety of cases. The inputs were modeled closer to those put forth in NRC Guide 1.190 in terms of the mesh tallies, as seen in **Table 6**.

Table 6: Inputs used for the full factorial DOE cases.

	Low	Middle	High
Particles	100,000,000	2,550,000,000	5,000,000,000
Shift Cores	100	225	400
Shift Axial	1	40	80
Shift Radial		15	
Shift Aximuthal	40	212	360
Unique Pins		off (-1)	
MPACT Axial	1	20	40

The radial and unique pins inputs were determined to be statistically unimportant in both the time and accuracy screening designs. Therefore, these two inputs were kept constant between both the time and accuracy testing. The number of tally regions was designed to abide close to the requirements set forth by the NRC as described following. Unique pins were decided to be used off to reduce the total run time and memory requirements of running the code. The number of cores used by the Shift calculation as well as the number of source regions were chosen such

that the total number of cores per run was maintained at a level feasible to industry sized

computers – approximately 1000 cores.

3.2.1 Analysis of Full Factorial Design for Time Output

A full factorial was used to perform more rigorous screening of the remaining inputs. Three

levels were used for the three remaining inputs, yielding a total of 27 runs. The values of inputs

used can be seen in **Table 7**. The values held constant for this set of runs was chosen to abide by

restrictions set forth by NRC Guide 1.190. Unique pins were turned off to reduce the amount of

memory used and to reduce overall runtime.

Table 7: List of inputs used for the full factorial design for the time component.

	Low	Middle	High
Particles	100,000,000	2,550,000,000	5,000,000,000
Shift Cores	100	225	400
Shift Axial		72	
Shift Radial		15	
Shift Aximuthal		320	
Unique Pins		off (-1)	
MPACT Axial	1	20	40

Once completed, the results for the time needed to complete the MC calculation were

entered into Minitab to perform analysis on the DOE. Minitab was again used to produce the

pareto chart and normal plot in addition to other plots to view the results.

First looked at was the pareto chart. **Figure 16** shows all the first order interactions as

well as secondary and tertiary. As can be seen, the least influential were those associated with the

number of MPACT levels. While this was included in this set of run cases, it was expected that it

would not be statistically important based off the screening results.
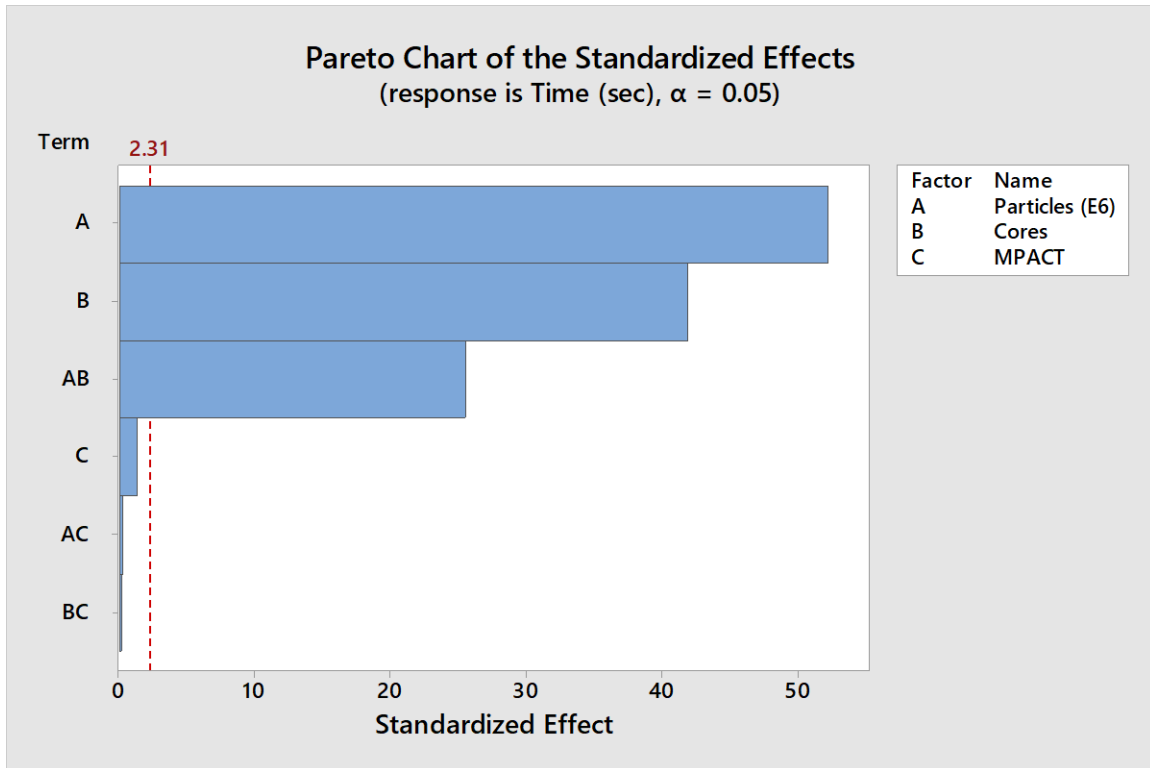
Figure 16: Pareto chart of full DOE for the time component.

Looking at a plot of the main effects gives insight on the way each level of the factor impacts the output. Shown in **Figure 17** is the main effects plot for the output of the Shift calculation time. The horizontal line across all three plots shows the mean run time in seconds for the Shift calculation. The horizontal axis shows the different levels for each of the inputs. Steeper slopes of the line indicate a larger magnitude of a main effect. From the graphs, it can be seen then largest increase occurs when increasing the number of particles, while increasing the number of cores used decreases the total time, though less and less as the number of cores increase. The number of source regions barely impacts the time required.
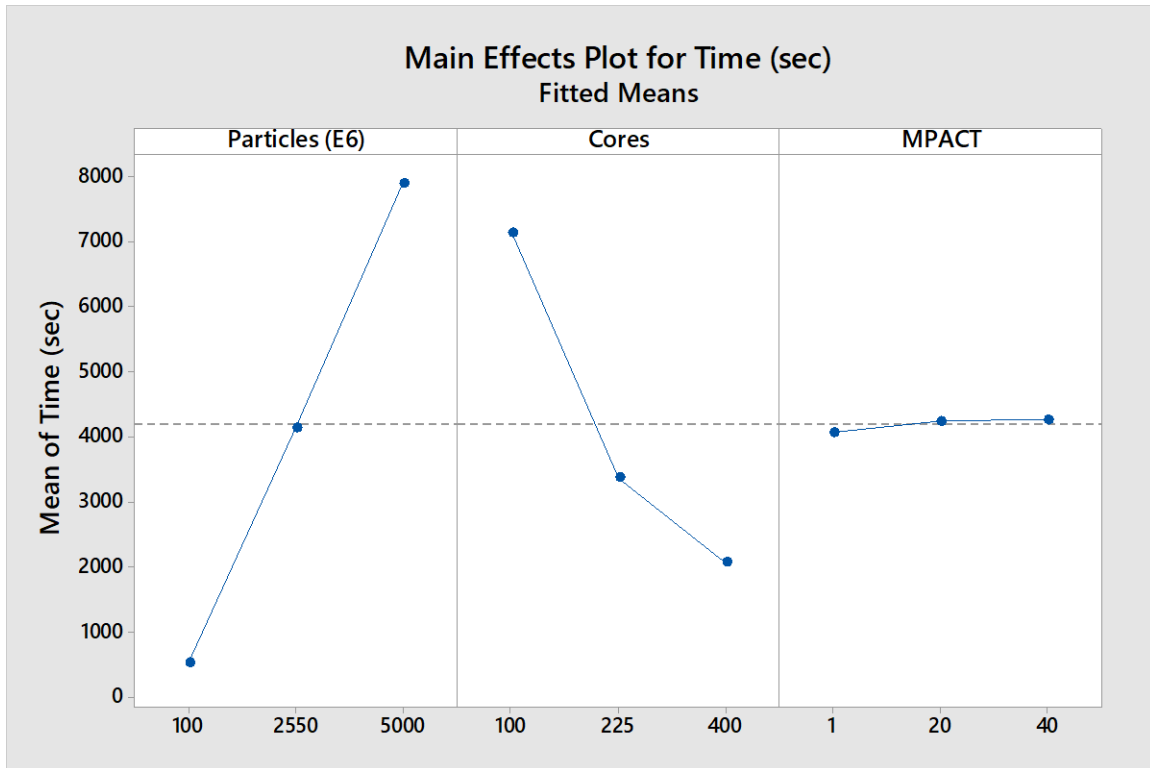
Figure 17: Main effects plot showing the way the time changes based off the different levels of each input.

Lastly, the residual plots, seen in **Figure 18**, were looked at to ensure that the modeling was appropriate to the data set. Residuals are a useful tool in analyzing how well a model fits a data set. A series of four plots was constructed: the normal probability plot, the versus fit plot, the histogram, and the versus order graph. The residuals versus order plot indicates the independence of the observations. When no detectable pattern is found, it is safe to assume that the residuals are independent from one another.
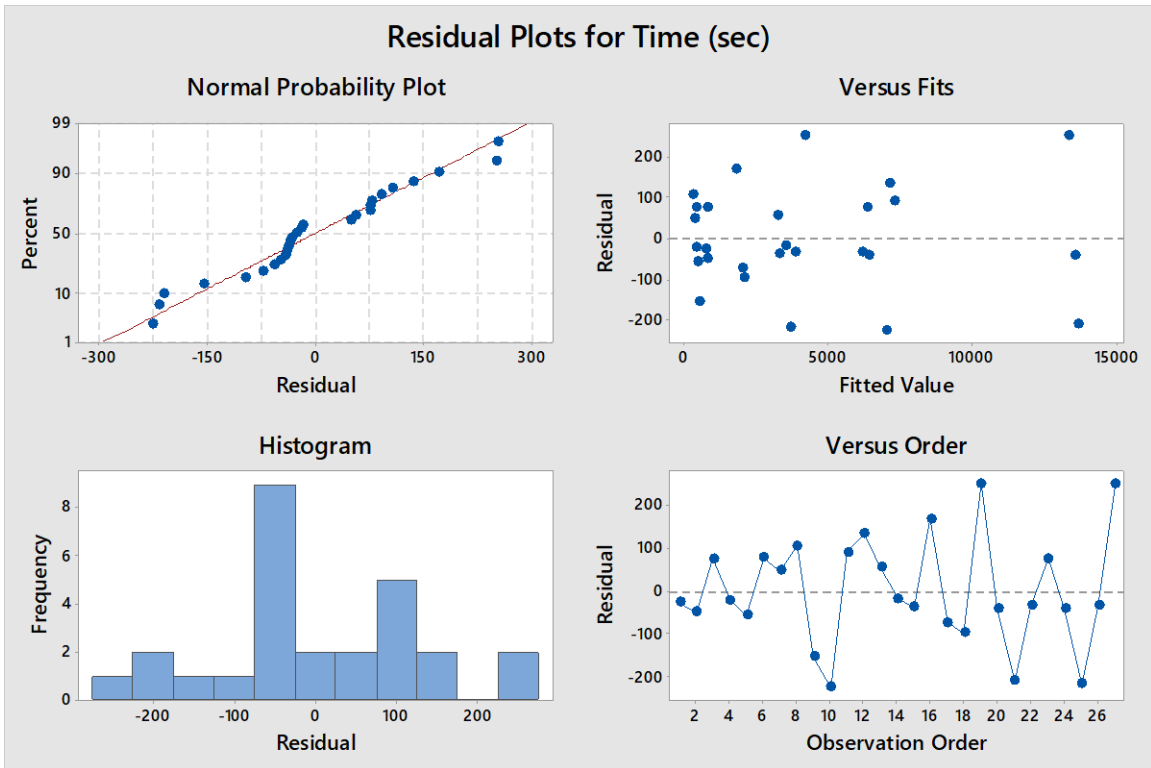
Figure 18: Four residual plots for the full DOE for the time component.

From looking at the normal probability plot and the versus fit plot, there are some outliers in the data set. These points occur when the points fall far away from either the line or from zero respectively. This breaks two assumptions of the linear regression model, making the interpretation of the data as is difficult and possibly unreliable. Additionally, it can be seen that the residuals do not follow an approximate normal distribution – another indication that the data may be difficult to interpret in its current form. The normal probability plot shows more of an inverted S-shape. This shape is indicative of a distribution with short tails – not so much a normal distribution. This can lead to inaccuracies in the confidence intervals as well as the p-values.

One tool for dealing with non-normal data is the Box-Cox transformation of data. When doing a Box-Cox transformation, a power function is used to transform the data to obtain a normal distribution with constant variance. This, for example, could be a logarithmic or

exponential function. The transformation can change the scale of the output though in addition to the calculated coefficients for the model. However, the data in the transformed space should abide by a normal distribution and should be able to be processed well and accurately by Minitab.

A Box-Cox transformation is done by determining a power transformation parameter, λ, and applying it to raw data. The estimation of this parameter is found by applying an algorithm to find a range over a maximum and minimum value that it could occur based off statistical fitness tests then selecting a value within that range that makes the most sense[31]. Once this value is determined, the transformation is performed according to equation (14)[31]:

$$y = \begin{cases} \dfrac{y_i^{\lambda} - 1}{\lambda}, & if \ \lambda \neq 0 \\ \ln y_i, & if \ \lambda = 0 \end{cases} \qquad (14)$$

Where i is the output for a given value, $i = 1, 2, …, n$, up to n number of runs. More precise information on the Box-Cox transformation can be found in reference 31. The methodology, including the seven fitness tests used to determine λ, and history of its development will not be discussed in this research, and will only be applied in the sense of Minitab performing the analysis to get the value of λ used in the transformation of the data.

A value of $\lambda=1$ is associated with using the original data. When the confidence intervals include 1, no transformation is required. However, when it is not, choosing an appropriate λ and therefore appropriate transformation is necessary to achieve normality. When a Box-Cox transformation analysis was performed on the Shift time data, the optimal λ value of 0.333467 was calculated for the data, which Minitab rounds to 0.5.

This optimal value of λ was used to perform a Box-Cox transformation on the original data so that a linear regression model could be accurately fit to it. The analysis was done using Minitab. By analyzing the residual plots created after the Box-Cox transformation, seen in **Figure 19**, it is observed that the assumptions necessary for regression modelling are met. The data is approximately normally distributed, and the residuals are still independent, though better and more equally spaced in the versus fit plot. There appear to be no major outliers in the set anymore and the residuals appear to abide by homoscedasticity.
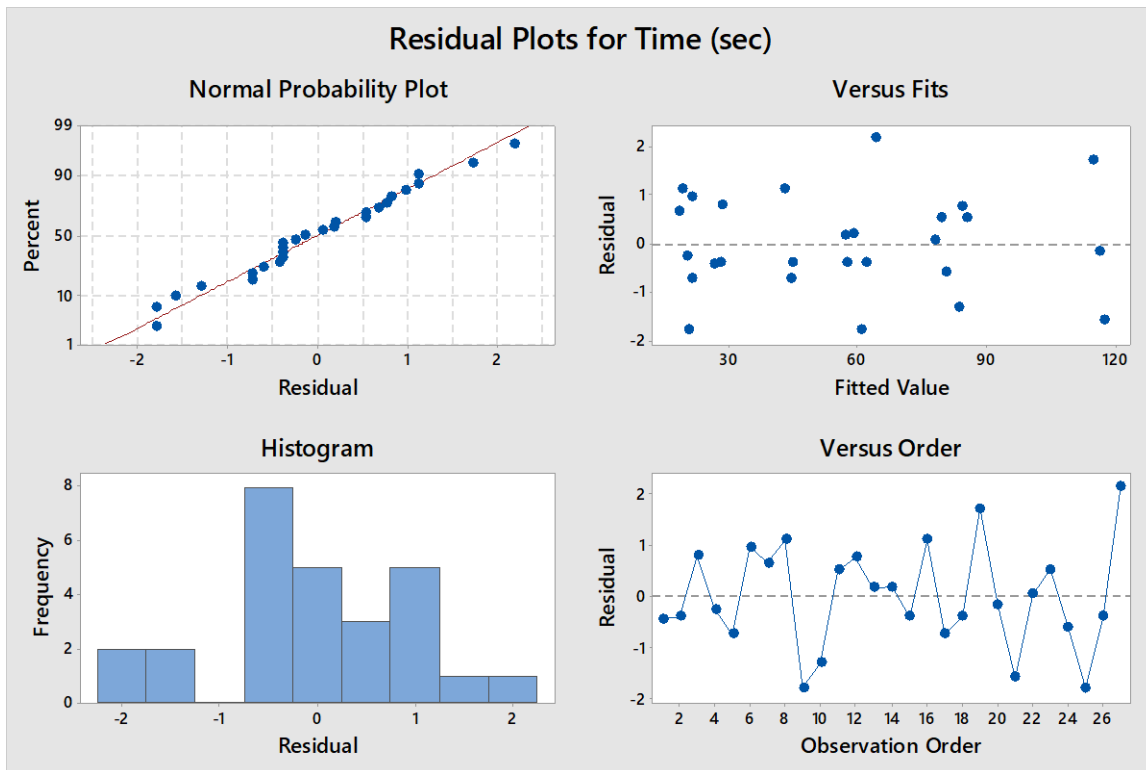
Figure 19: Residual plots for the transformed time output.

Looking at the information provided in the model summary table sheds more light on the benefit of transforming the data. The original set of data has a high S value and a low predictive R^2 value. This indicates a high standard deviation and low predictive power of the model. However, the transformed response yields a much smaller standard deviation and a much more powerful predictive equation. The R^2 value, the percent of variance explained by the model, also

increases from the original to the transformed data. These conclusions create support for the

model created by the transformed data as being statistically sound.

3.3.2 Analysis of Full Factorial Design for Accuracy Output

A full factorial design was used to perform more rigorous screening. Three levels were used for

the four remaining inputs, yielding a total of eighty-one runs. The values of inputs used can be

seen in **Table 8**. The values held constant for this set of runs was chosen to abide closely to the

restrictions set forth by NRC Guide 1.190. Unique pins were turned off to reduce the amount of

memory used and to reduce overall runtime.

Table 8: List of inputs used for the full factorial design for the accuracy component.

	Low	Middle	High
Particles	100,000,000	2,550,000,000	5,000,000,000
Shift Cores		400	
Shift Axial	1	40	80
Shift Radial		15	
Shift Aximuthal	1	212	360
Unique Pins		off (-1)	
MPACT Axial	1	20	40

The pareto chart in **Figure 20** shows all the first order interactions as well as secondary

and tertiary. From this chart, most of the factors seem to be statistically important to the output,

while those interactions that were unimportant were removed. **Figure 21** shows the residual plots

for the same cases. Unlike the time cases, the results abide by the seven assumptions of

regression analysis, and therefore do not need any transformations done on them in order to draw

conclusions on the results.
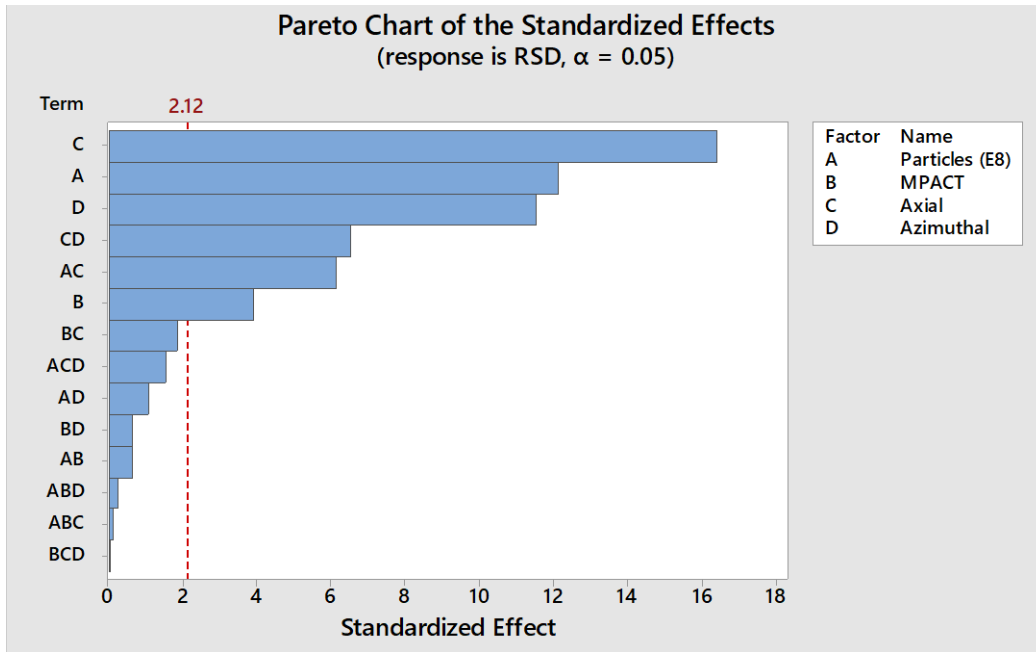
Figure 20: Pareto chart showing the results for the full DOE for the accuracy component.
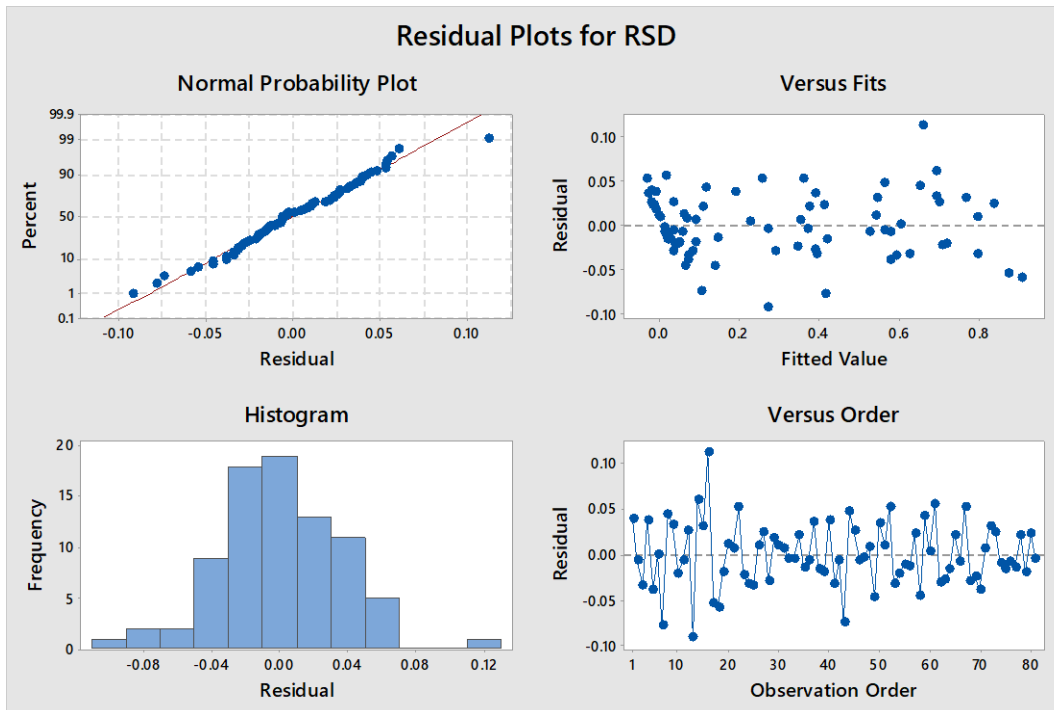
Figure 21: Residual plots for the full DOE for the accuracy component.

Looking at a plot of the main effects gives insight on the way each level of the factor actually impacts the output. Shown in **Figure 22** is the main effects plot for the output of the RSD. The horizontal line across all three plots shows the RSD as a decimal. The horizontal axis shows the different levels for each of the inputs. Steeper slopes of the line indicate a larger magnitude of a main effect. From the graphs, it can be seen then largest decrease occurs with increasing particle histories while the number of axial tally regions seems to create the largest increase in the RSD. The number of MPACT source regions seems to have only a nominal effect on the RSD in comparison to the rest of the inputs.
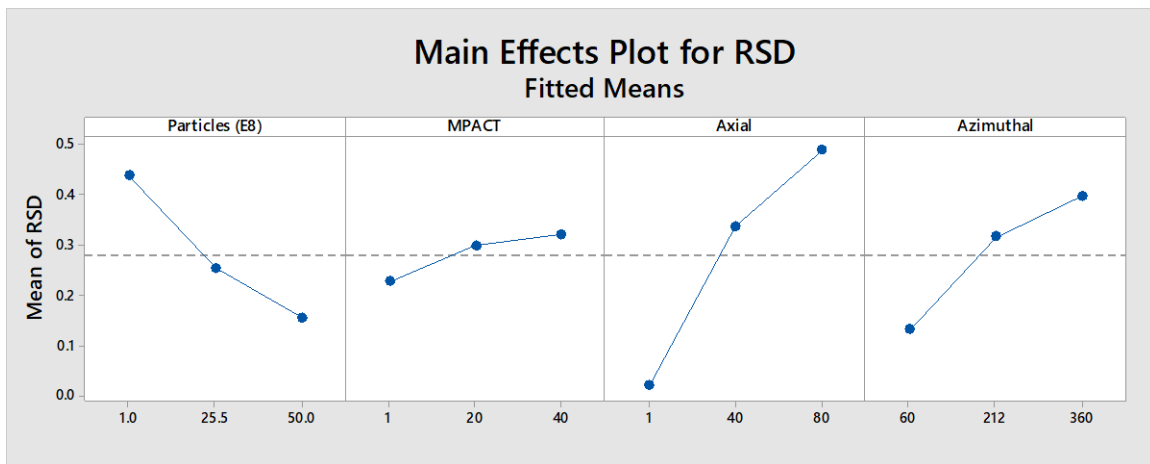
Figure 22: Main effects plots for the full DOE for the accuracy component.

3.3 Creating a Model

The object of this research is to test and model the output performance of the VERAShift code. All the previous testing was collected and used to produce a suite of cases used to model the performance to be in accordance with the NRC guidelines put forth by Guide 1.190. As previously mentioned, this includes having appropriately sized tally regions in addition to reaching a certain accuracy of the result. Companies, however, do not have unlimited resources, and therefore, a tradeoff between the best estimate and the licensing acceptable values must be considered. While a minimum value is set forth by Guide 1.190, this does not necessarily mean

that this would be the best estimate of the fluence if, say, the size of the tally region was reduced

or the accuracy was increased. To account for this, the cases were ran using the NRC guidelines

as the limiting values and increasing those to be more refined.

3.3.1 Analysis of Source Region Size

Further investigation into the number of VERAShift tally regions yields information on the

sensitivity of the absolute fluence value to the source regions themselves. Looking at a series of

cases that all contain the exact same input specifications except for the number of source regions,

as seen in **Table 9**, from 1 to 40 VERA axial levels results in a 33% difference in the absolute

fluence value. In other words, the fluence predicted by 1 axial level is an underprediction of that

found by using 40 axial levels. From this, it can be safely assumed that using anything less than

40 axial levels in VERA will lead to an inaccurate RSD values due to improper source averaging

in the VERA source regions. Because of this, the number of VERA source regions was

eliminated as a dependent variable for the RSD and instead replaced with the constant value of

40 axial levels.

Table 9: Comparison of maximum fluence values for different source region sizes in the VERA calculations.

	Particles	Axial	Azimuthal	MPACT	Max Fluence	Difference
Case 1	5 Billion	80	360	1	1.1106E+08	---
Case 2	5 Billion	80	360	20	1.2621E+08	13.64%
Case 3	5 Billion	80	360	40	1.4740E+08	32.71%

3.3.2 Analysis of P_N Order on Monte Carlo Performance

For the CADIS method, it was desired to see the impact that the P_N order had on the maximum

fluence value for a fixed number of particle histories. Intuitively, increased P_N order (and hence

accuracy) in the adjoint calculation should result in improved source biasing for the Shift calculation. A higher order used allows for higher moment of the scalar flux to be calculated resulting in more accurate scattering distributions, and therefore, more accurate transmission of particles. This is seen in **Figure 23** and **Figure 24**.
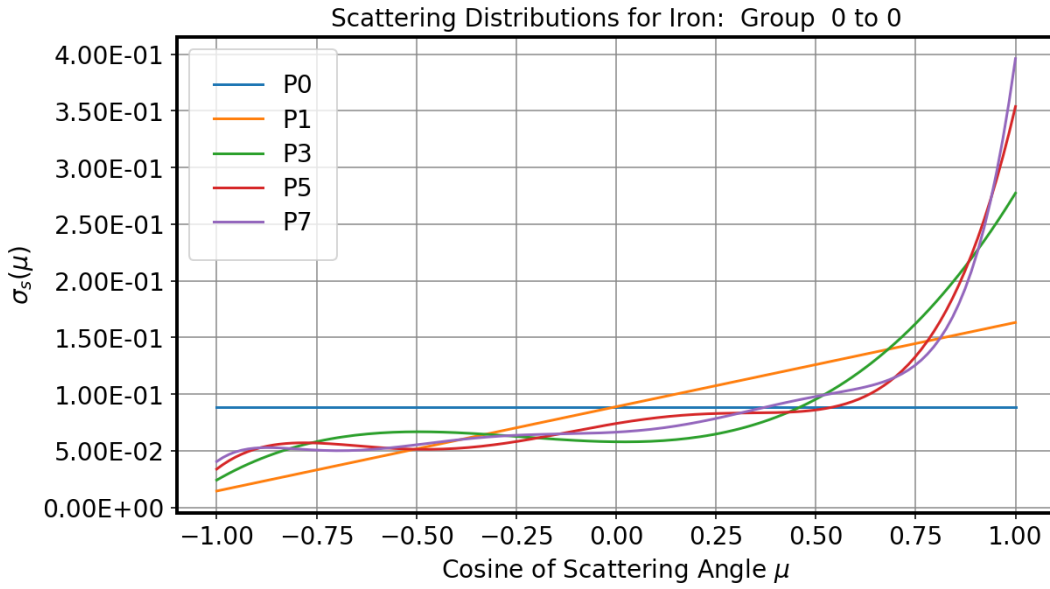
Figure 23: Scattering distributions in iron of different PN orders for in group scattering [34].
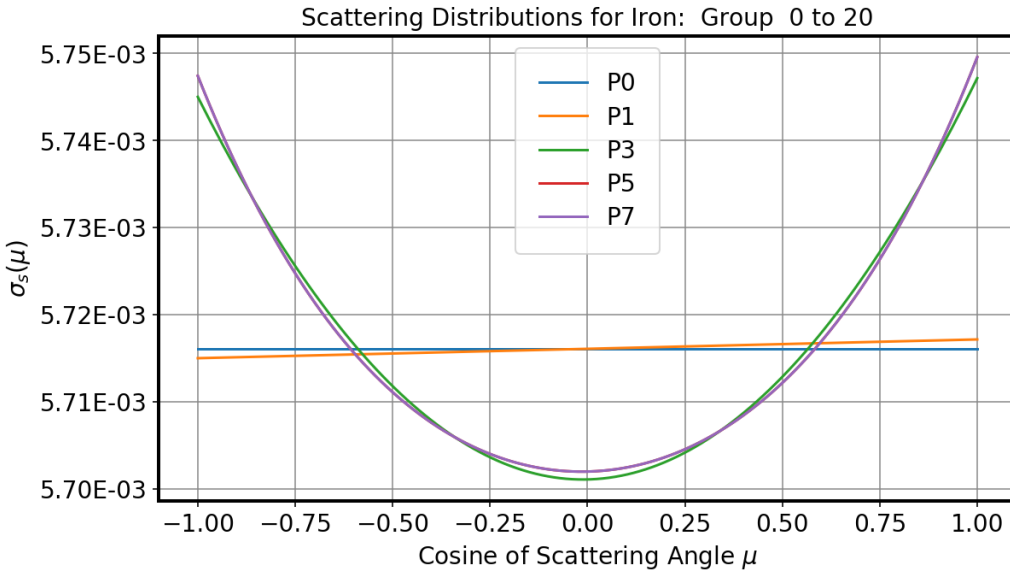
Figure 24: Scattering distributions in iron of different P_N orders for group to group scattering [34].

The adjoint calculation takes place after the VERA calculation and is used for determining the source biasing map, an integral part of the hybrid method. While this calculation does not need to be super precise, greater precision in the value would make more a better biased source map, which would lead to greater accuracy in the final fluence values.

The P_N order is an input under the Shift block in the input which determines the order of the P_N equation used during the adjoint equation. Increasing the P_N order for the calculation does increase the memory requirements of the calculation and scales by $(n+1)^2$. Therefore, using P_3 would require sixteen times the amount of memory as P_0. The amount of memory required for the total execution of the code is a current issue within the program that is actively being worked on. Due to these limitations, the maximum P_N order that could be successfully executed is P_5, and this was only accomplished for a less refined core model.

The initial release of VERAShift, as was discovered during this research, discovered an error in the CADIS method implementation. The error truncated the adjoint calculation to the inner core barrel instead of past the vessel and onto excore regions. Therefore, the biasing focused on the barrel and not the vessel. **Figure 25** below shows the effect of the P_N order on the fluence. From this graph, it is seen that the maximum fluence is independent of P_N order which is unexpected. This could be the result of the CADIS error. The maximum fluence however is nevertheless within the error bars and therefore does not depend on the P_N order.
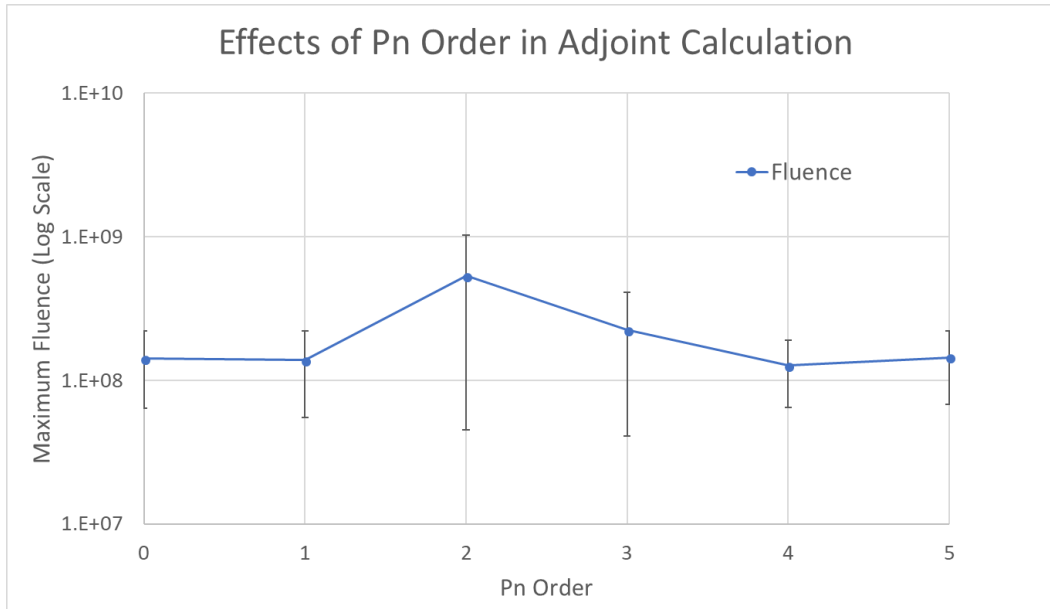
Figure 25: Maximum fluence and associated standard deviation for varying P$_N$ orders.

3.3.3 Model of Time Component

From the results above, the number of VERA source regions does not impact the overall time taken to perform the MC calculation. The main two inputs effecting the time component are, as expected, the number of particles transported, and the number of cores used to perform the calculation. As seen in **Figure 17**, the time increases nearly linearly with increasing number of particles. The time decreases in an apparently asymptotic way with increased number of cores.

Looking at the results of the first few cases run in the secondary screening for the time component, the average decrease in time from 100 to 225 cores is approximately 330 seconds. Going from 225 to 400 cores, the decrease is only approximately 60 seconds, five and a half times less than the previous increase. Assuming this trend were to continue, increasing to 625 cores would likely only reduce the run time by approximately 10 seconds compared to using 400 cores. These time estimates are only for a single state point. For a depletion, it could take as many as 60 state points. Taking this into account, the amount of time saved going from 100 to

225 cores would be nearly five and a half hours, from 225 to 400 cores would be one hour, and

from 400 to 625 would be approximately 10 minutes. Therefore, for the most effective use of

computational resources, 400 cores is an appropriate number of cores to run on. Using more than

this does not reduce the time by a significant amount and would only take up more resources

than may be available. Because of this, 400 cores was used as the number of cores used and the

value with which the model was created with. The levels used for all inputs can be seen in **Table

10**. The values were chosen with the attempt to make all RSD values less than 20% to abide by

the NRC guide, but also leave room to refine the tally regions if desired and still be able to apply

the model accurately.

Once completed, the values of time for each case were put into Minitab where a linear

regression was performed due to the dependence on only one variable – the number of particles.

This regression analysis was used to produce a model equation based on the output values. The

model for the time can be found in equation (15).

$$Time\ (sec) = 9699 + 0.5657\ x$$
$$Where\ x = number\ of\ particles\ (\cdot 10^6)$$

(15)

The model is created with 95% confidence limits, which are illustrated in **Figure 26** for a

list of sample inputs values.

Regression for Time vs Particles (E6)
Prediction Report

Y: Time
X: Particles (E6)

Prediction Plot
The red fitted line shows the predicted Y for any X value. The blue dashed lines show the 95% prediction interval.

X	Predicted Y	95% PI
-20000	-1614.7	(-62609, 59380)
-10000	4042.3	(-56183, 64267)
0	9699.2	(-49815, 69214)
10000	15356	(-43509, 74221)
20000	21013	(-37265, 79291)
30000	26670	(-31086, 84426)
40000	32327	(-24973, 89627)
50000	37984	(-18929, 94897)
60000	43641	(-12954, 100236)
70000	49298	(-7049.8, 105646)
80000	54955	(-1217.4, 111127)
90000	60612	(4542.8, 116681)
100000	66269	(10230, 122307)
110000	71926	(15845, 128007)
120000	77583	(21387, 133779)
130000	83240	(26856, 139623)
140000	88897	(32254, 145539)
150000	94553	(37582, 151525)
160000	100210	(42840, 157581)
170000	105867	(48030, 163705)
180000	111524	(53154, 169894)
190000	117181	(58214, 176149)
200000	122838	(63211, 182466)
210000	128495	(68147, 188843)
220000	134152	(73026, 195279)

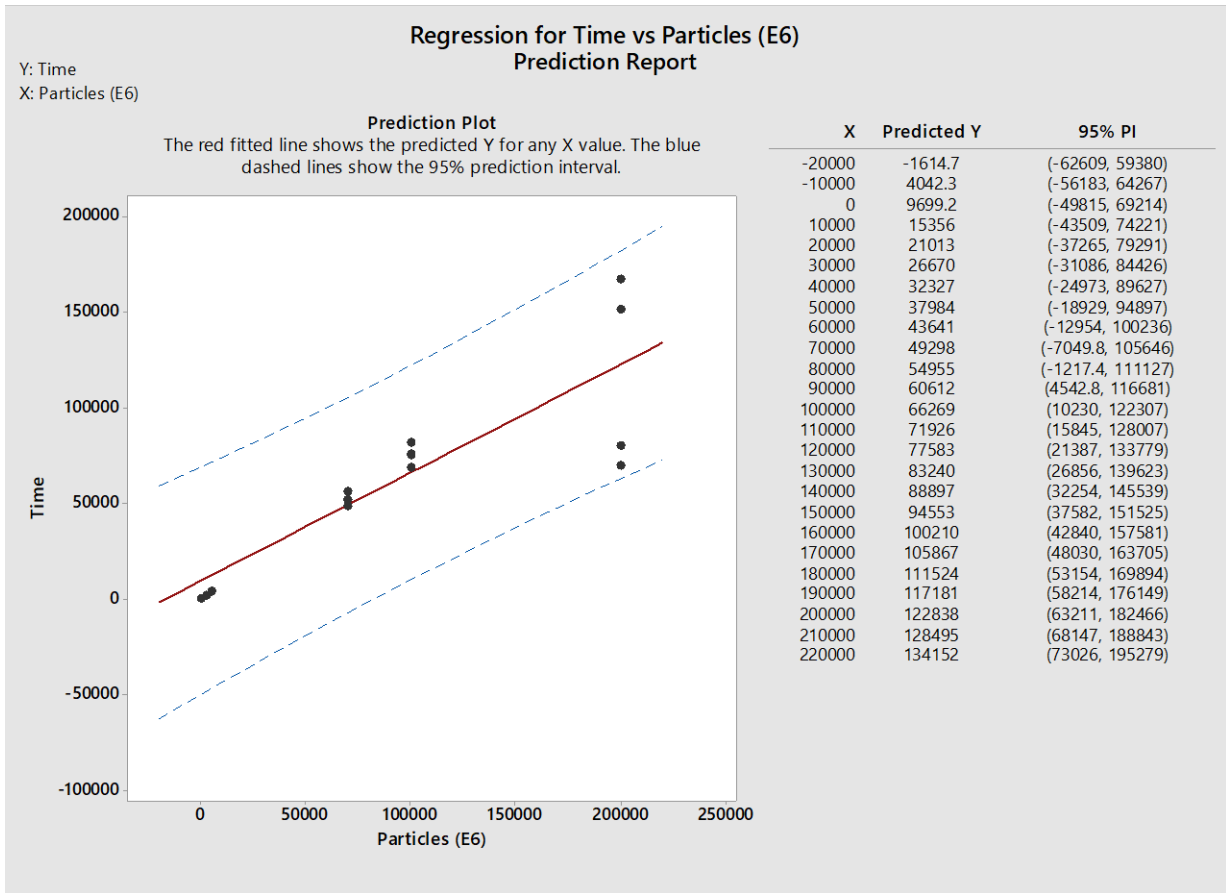**Figure 26: Model for the time component. Shown are several example inputs and the resulting line in addition to the confidence intervals.**

3.3.4 Model Accuracy Component

As discussed in section 3.3.1, the number of VERA source regions was held constant for these test cases to ensure the best estimate is achieved. The levels of the inputs can be seen in **Table 10** in the previous section.

Table 10: Values used for the modeling cases.

	Low	Middle	High
Particles	70 Billion	100 Billion	200 Billion
Shift Cores		400	
Shift Axial	72		108
Shift Radial		15	
Shift Aximuthal	320		480
Unique Pins		off (-1)	
MPACT Axial		40	

Like the screening design, a Box-Cox transformation was used to make the raw data abide by the seven requirements of regression analysis. The optimal value of lambda for this was determined to be -0.832078, which Minitab rounds to -1 in practice. Looking at the pareto chart in **Figure 27**, it can be seen that the number of azimuthal regions is deemed to be far less influential on the final RSD than initially presented in the screening design. The residuals plot in **Figure 28** demonstrates the necessary requirements for the regression analysis and modeling to proceed. The model equation can be seen in equation (16).
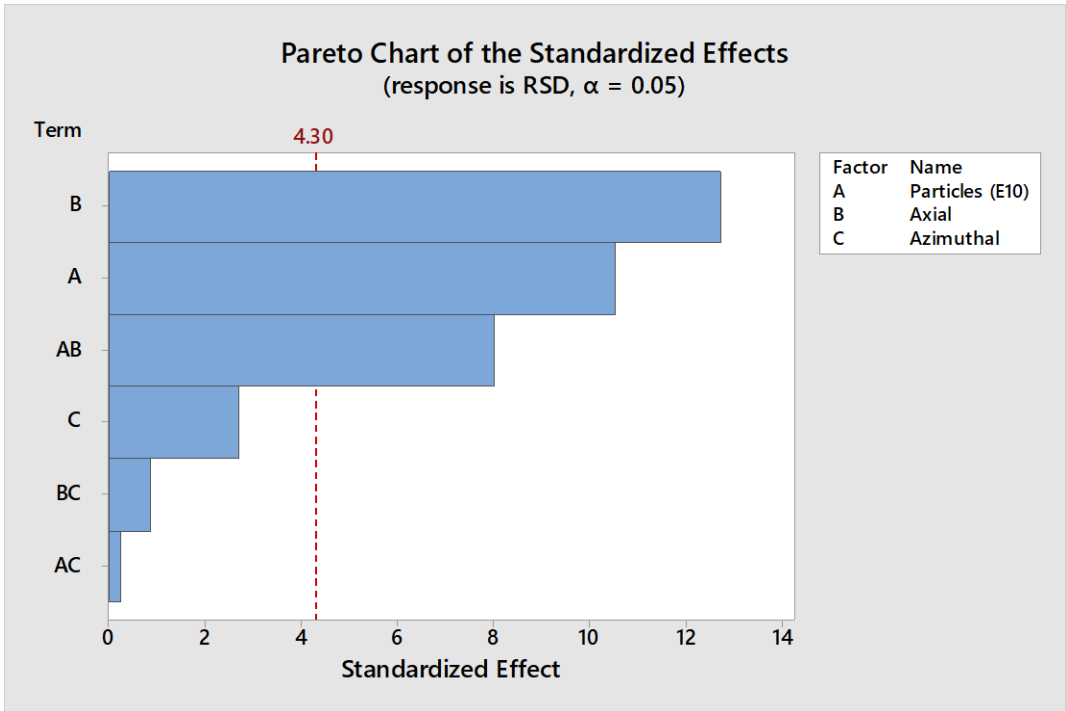
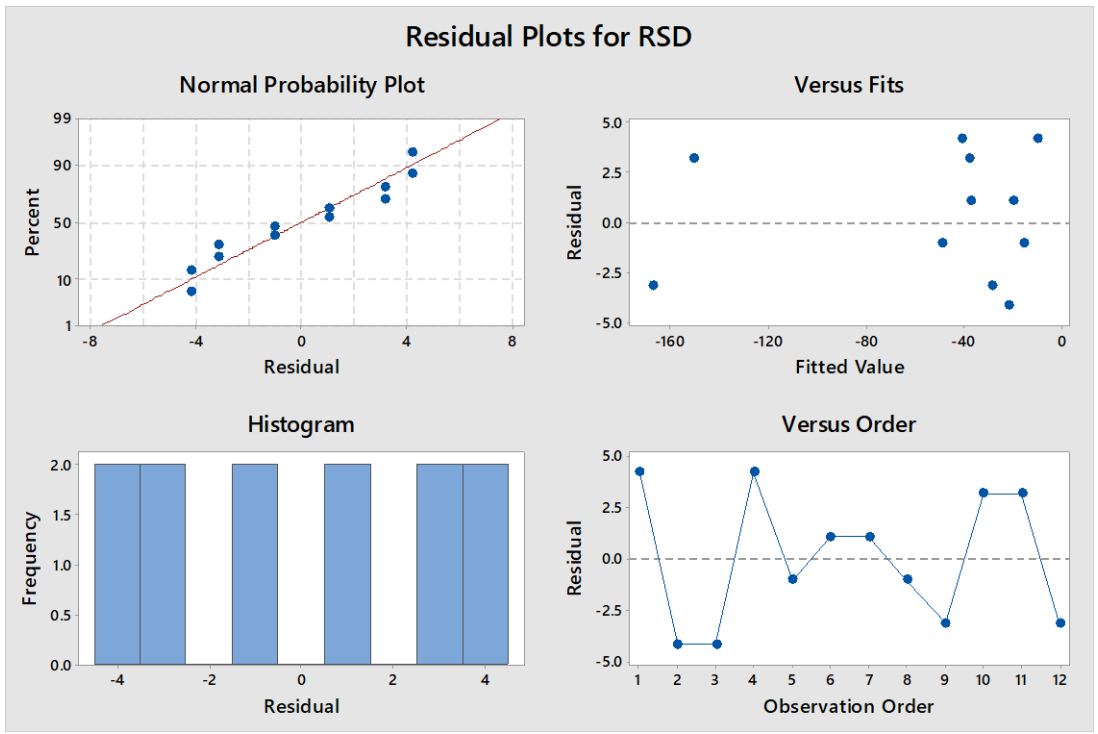**Figure 27: Pareto chart for the accuracy component for the final model.**

Figure 28: Residuals plot for the accuracy component for the final model.

$$Transformed\ RSD$$
$$= 74.2 - 18.89\ x_1 - 0.3368\ x_2 + 0.33\ x_3 - 0.331x_1^2 + 0.05558\ x_1 x_2 \qquad (16)$$
$$Where\ x_1 = number\ of\ particles\ (\cdot 10^{10})$$
$$x_2 = number\ of\ axial\ regions$$
$$x_3 = number\ of\ azimuthal\ regions$$

The model is created with 95% confidence limits with the RSD as a decimal, not a

percent. It should be noted that this equation is in terms of the transformed output and resides

within transformed space. Therefore, for it to be correct, the transformation must be undone for

an accurate comparison of outputs. The transformation can be undone by following the equations

set forth in equation (14).

3.4 Testing Equations

The equations produced in section 3.3 were used to predict the behavior of the code using a

series of test cases. These cases can be seen in **Table 11**.

Table 11: Values for the test cases used for comparison to the model equations.

	Particles	Axial	Azimuthal	MPACT	Cores	Radial
Case 1	80 Billion	90	360	40	400	15
Case 2	137 Billion	75	360	40	400	15
Case 3	119 Billion	100	360	40	400	15
Case 4	70 Billion	85	360	40	400	15

These cases were ran and the results were compared to the values calculated using the

model equations set forth in sections 3.3.3 and 3.3.4. The results from the actual and predicted

times were plotted as a function of how many hours were taken to complete the single state point

MC calculation. The RSD values were graphed as a function of percent, not decimal. These two
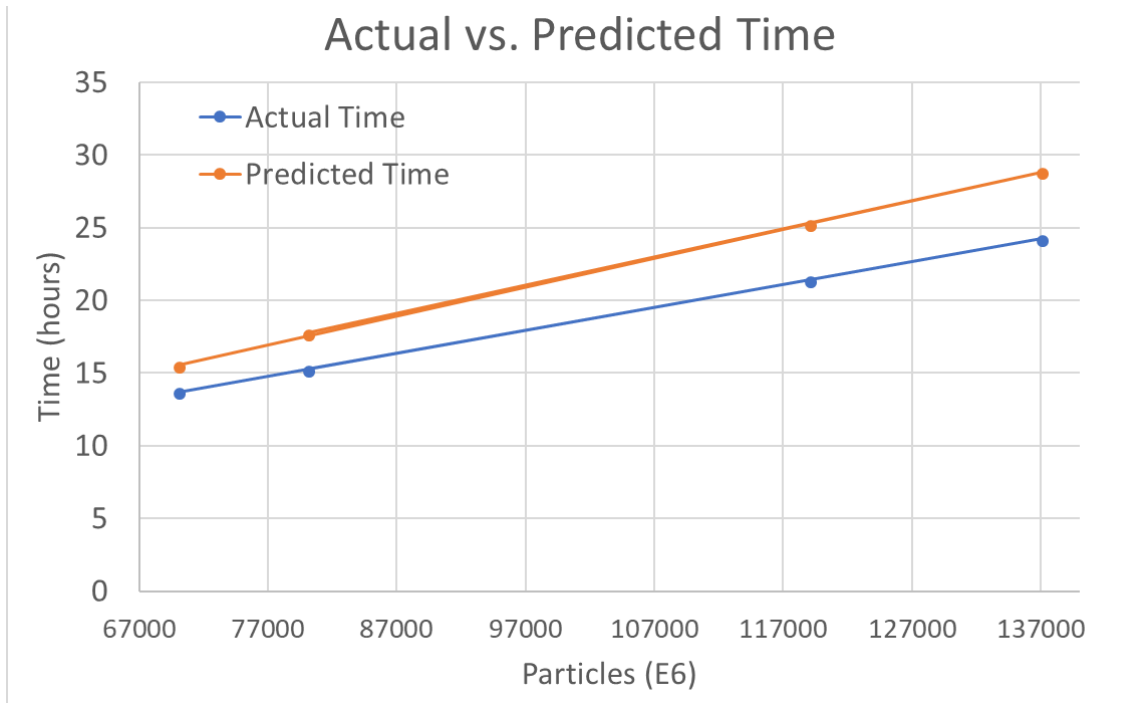
graphs can be seen in **Figure 29** and **Figure 30**.

Figure 29: Graph showing the actual and predicted run times for the MC calculations.
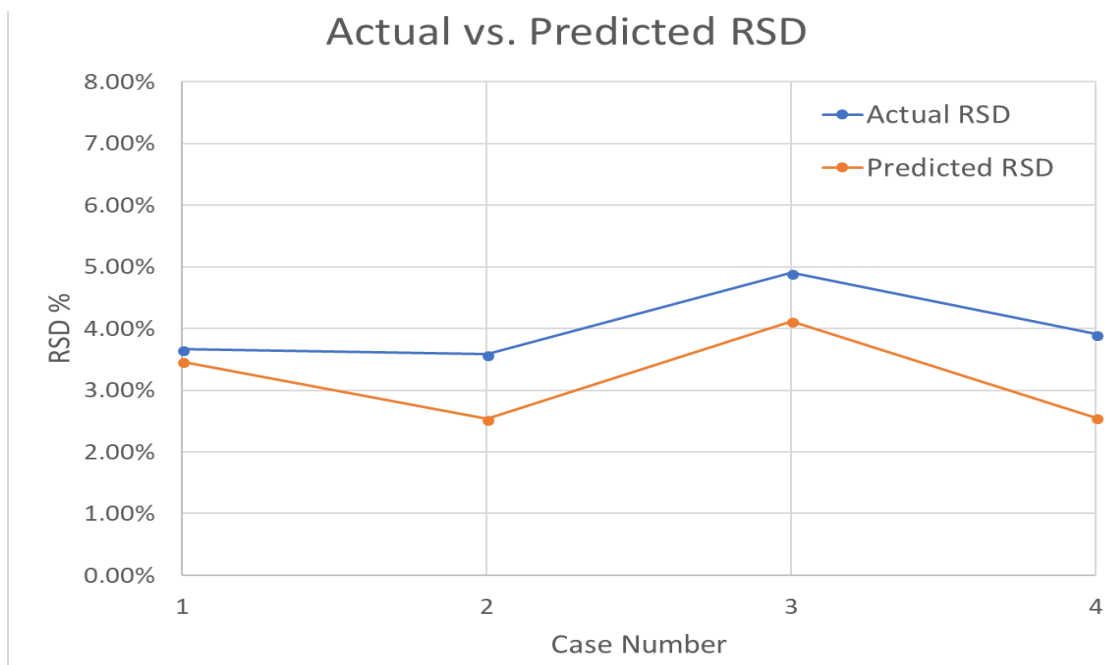

Figure 30: Graph showing the actual and predicted RSD value.

The model results demonstrate the ability to predict the behavior of the VERAShift code. For instance, a company could interpolate that for a 1% RSD with minimum tally regions, they would need to run 190 billion particles, and this would run for approximately thirty-two and a half hours per state point using 400 cores. Being able to accurately model this behavior removes the guess work in determining what inputs would be necessary and the computing resources necessary.

The equations presented in this research were produced using only a small fraction of the total inputs available to VERAShift. They rely on ones deemed most influential to the output via the screening designs, though that is not to say that some important interaction could have been missed by not including a variable that was decided to be unimportant on its own. The data does meet all the requirements for the application of linear regression, thus making the model mathematically sound. In addition to adding more factors into the modeling, the sample sizes for test cases could always be increased to produced more reliable regression models. Increasing the number of cases run or by running a set of replicate test cases could further improve the accuracy of these equations. Larger sample sizes would provide a more precise estimate of the relationship between inputs and outputs, and, would therefore, produce models with higher R^2 values.

The cases used to build the models in this research all use tally regions that meet a minimum standard set forth by NRC Guide 1.190. These cases use the minimum number of values for the model's core dimensions and increases the refinement by 50% for the sake of obtaining a more true "best estimate" value. It should be noted that the minimum standard yields an average maximum fluence of 8.33E7 ± 2.73%, while the most refined case used produces an average maximum fluence of 8.65 ± 16.72% for seventy billion particles and 8.18E7 ± 0.59% and 8.32E7 ± 3.13% for the respective cases using 200 billion particles. This equates to a percent

difference of 3.83% and 1.65% for the respective number of particles for a 50% increase in refinement of tally regions. It can therefore be concluded that for adequate results, one need not go beyond the minimum standards for tally regions to get a best estimate value that meets the accuracy requirement of the NRC.

It should be noted that the radial tally region input does not appear in either of the postulated formulas, despite initially being considered an important factor. Looking at the location of where the maximum fluence occurs gives insight as to why this is. For the 81 cases ran for the accuracy component, every case had the maximum fluence occur at the same radially location – 219.71 cm. This corresponds to the inner radius of the vessel which is where the maximum fluence was expected. Therefore, it was determined that, for the fluence calculation, it is important that this tally region be sufficiently small to achieve decent statistics and the best possible estimate of the fluence.

Two of the model cases – the least refined/least particles and most refined/most particles cases – were visualized using VERAView. Using VERAView, several views of the fluence could be illustrated. The first set of images show the show the normalized pin powers and vessel fluence. The pin powers are normalized to the core averaged heat flux and the fluence is in units of neutrons per cm^2. The normalized pin powers and the fluence are shown with different color scales to show differing values. The highest fluence is along the diagonal of the quarter core, where the fuel is nearest to the vessel, as would be expected. The next set of images show the axial view of the fluence along the entire vessel.

pin_powers: Axial 287.805, vessel_tally/fluence (flux/mean) at 287.805, exposure 0
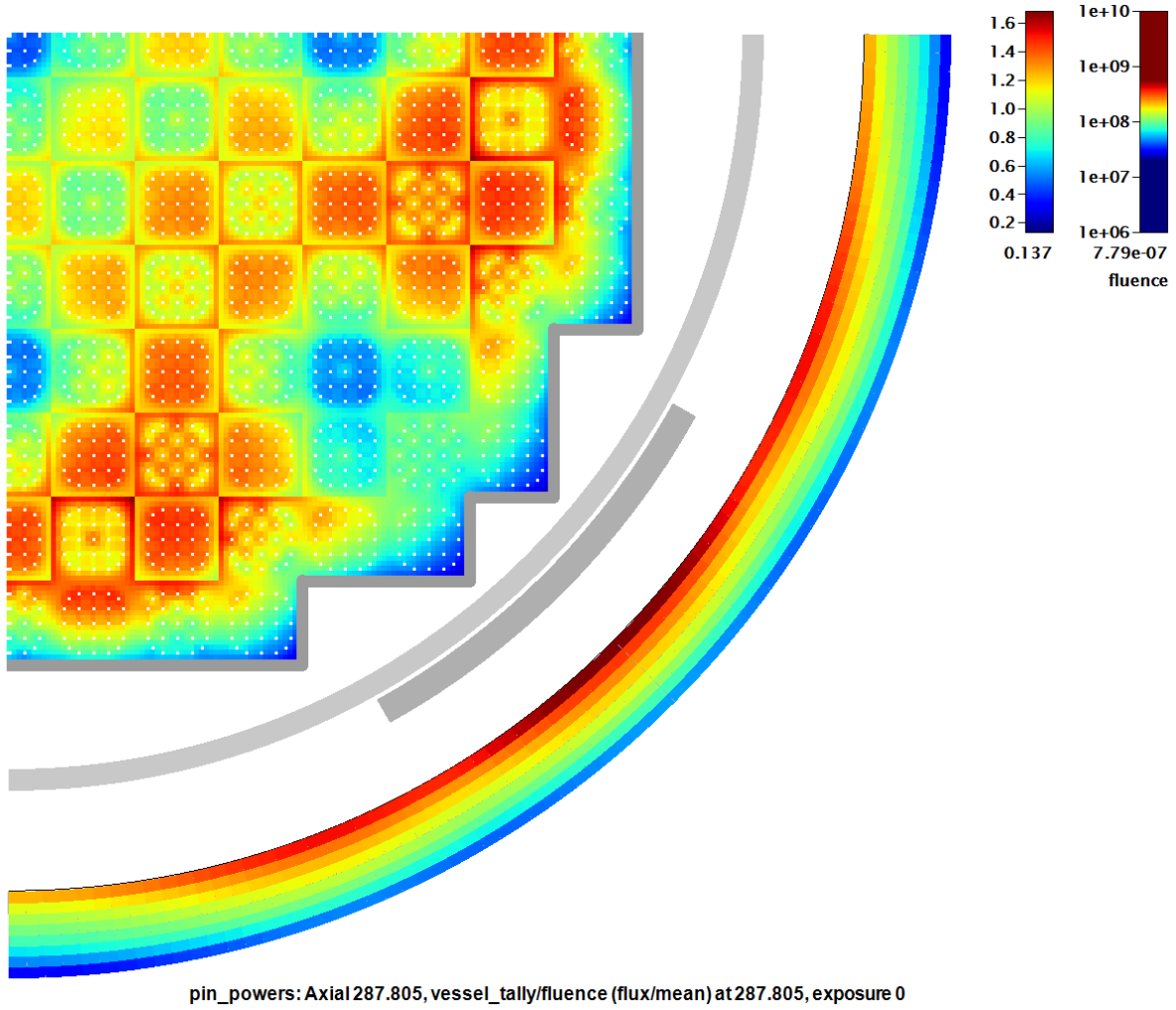
Figure 31: Core view for the fluence produced using VERAView for the least refined/least particles case.

pin_powers: Axial 290.352, vessel_tally/fluence (flux/mean) at 290.352, exposure 0
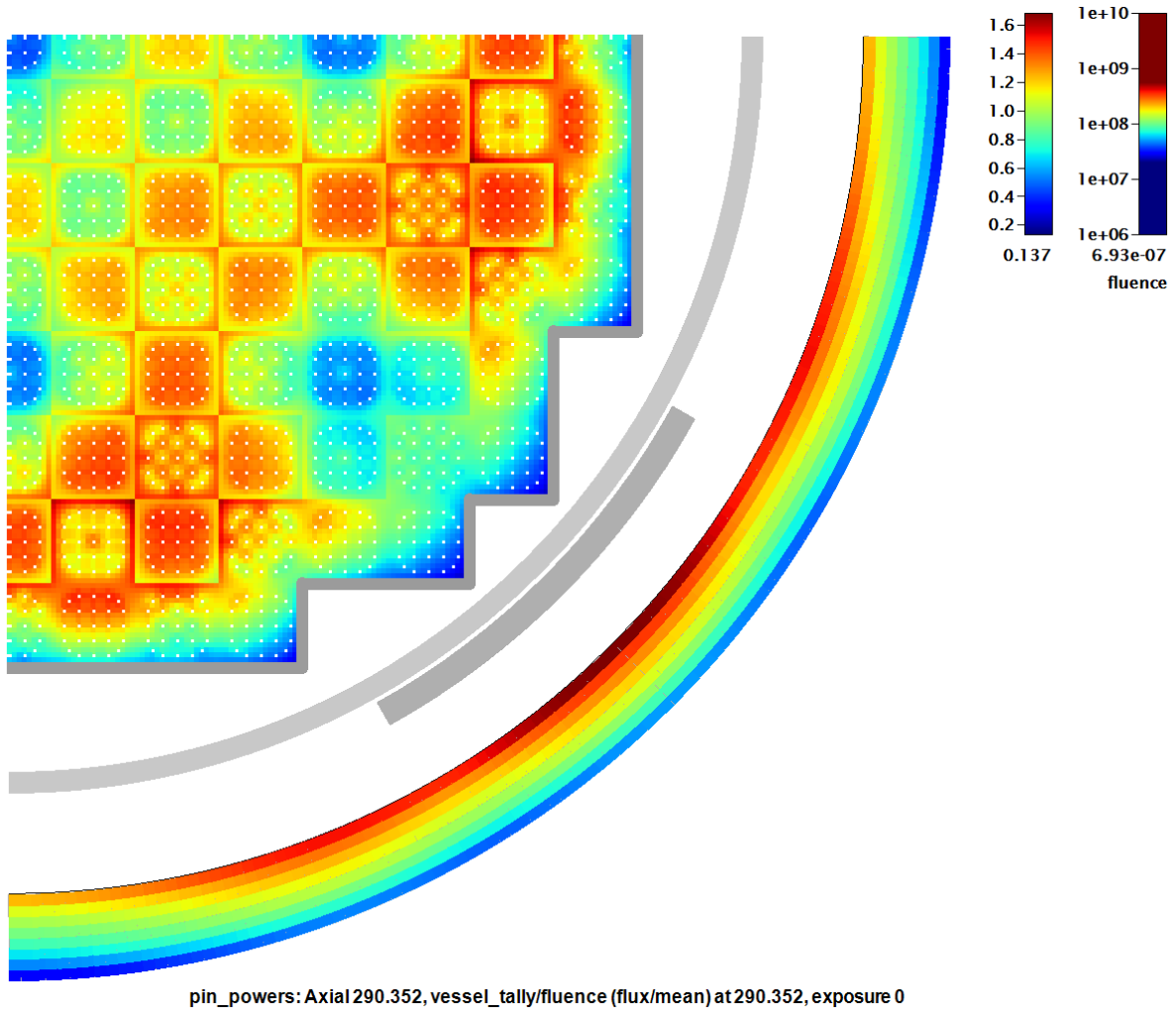
Figure 32: Core view for the fluence produced using VERAView for the most refined/most particles case.

pin_powers: vessel_tally/fluence (flux/mean), th=44 deg, exposure 0
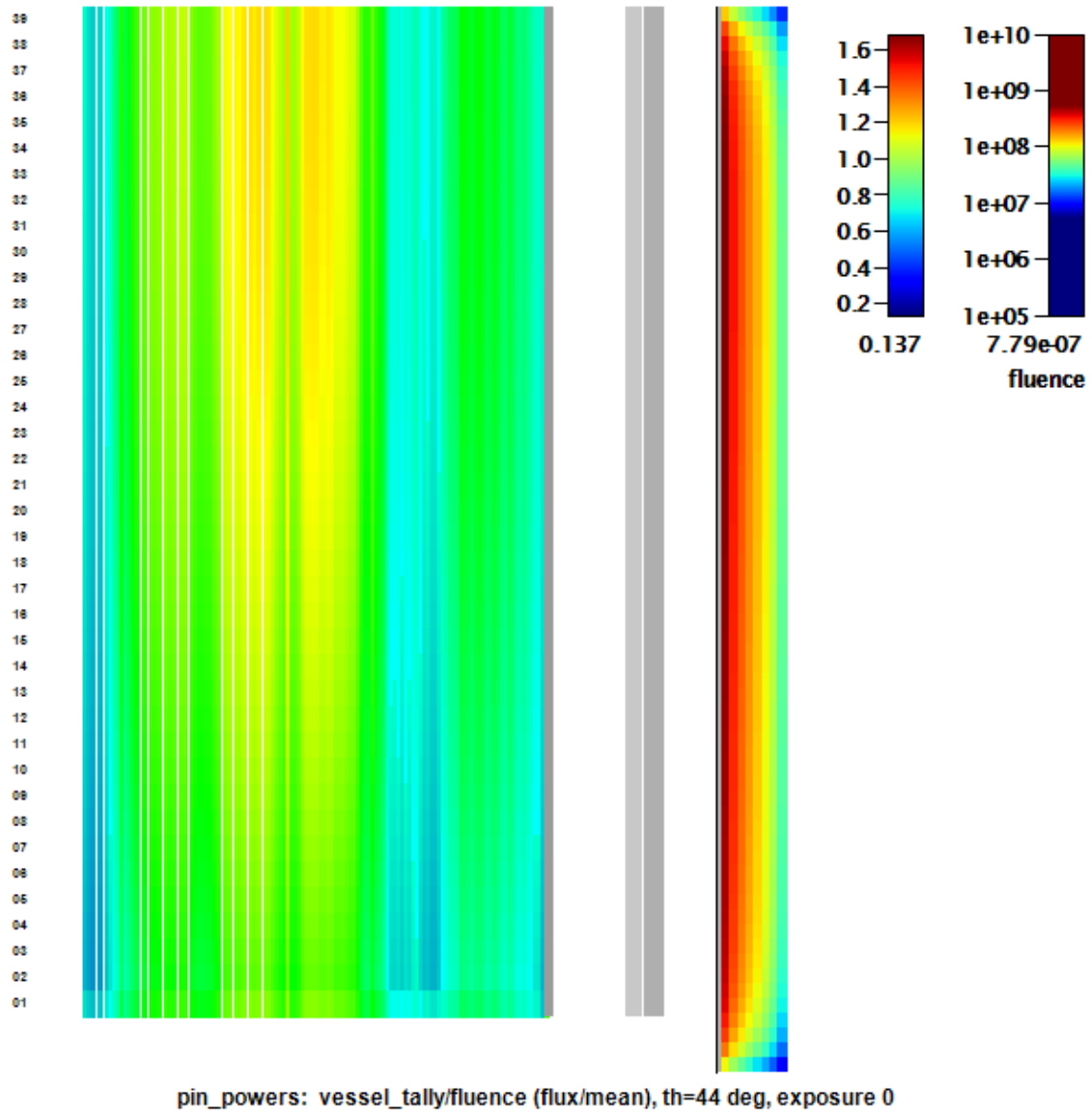
Figure 33: Axial view of the core produced using VERAView for the least refined/least particles case.
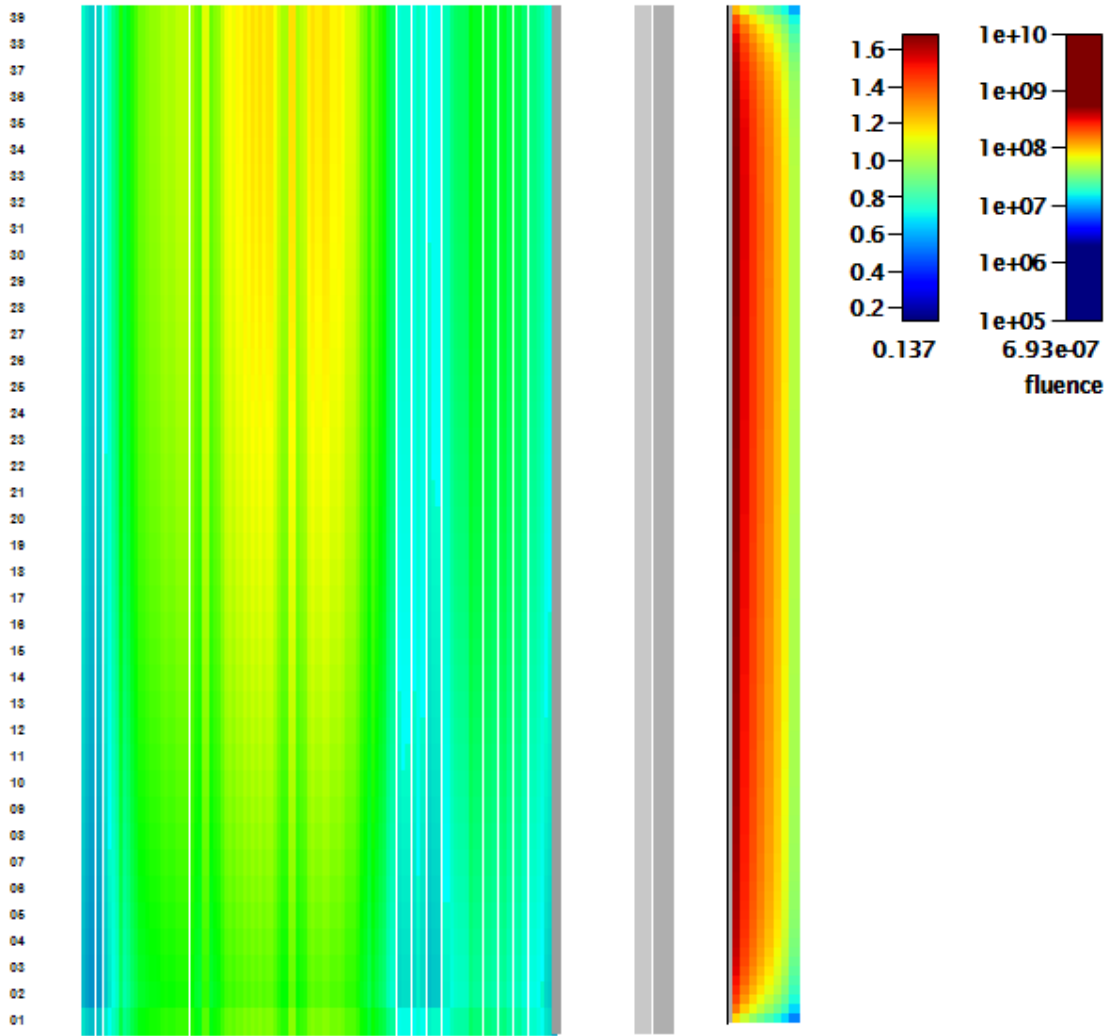
pin_powers: vessel_tally/fluence (flux/mean), th=43 deg, exposure 0

Figure 34: Axial view of the core produced using VERAView for the most refined/most particles case.

Figure 35: Plot showing the pin power axial distribution and axial fluence profile produced using VERAView for the least refined/least particles case.
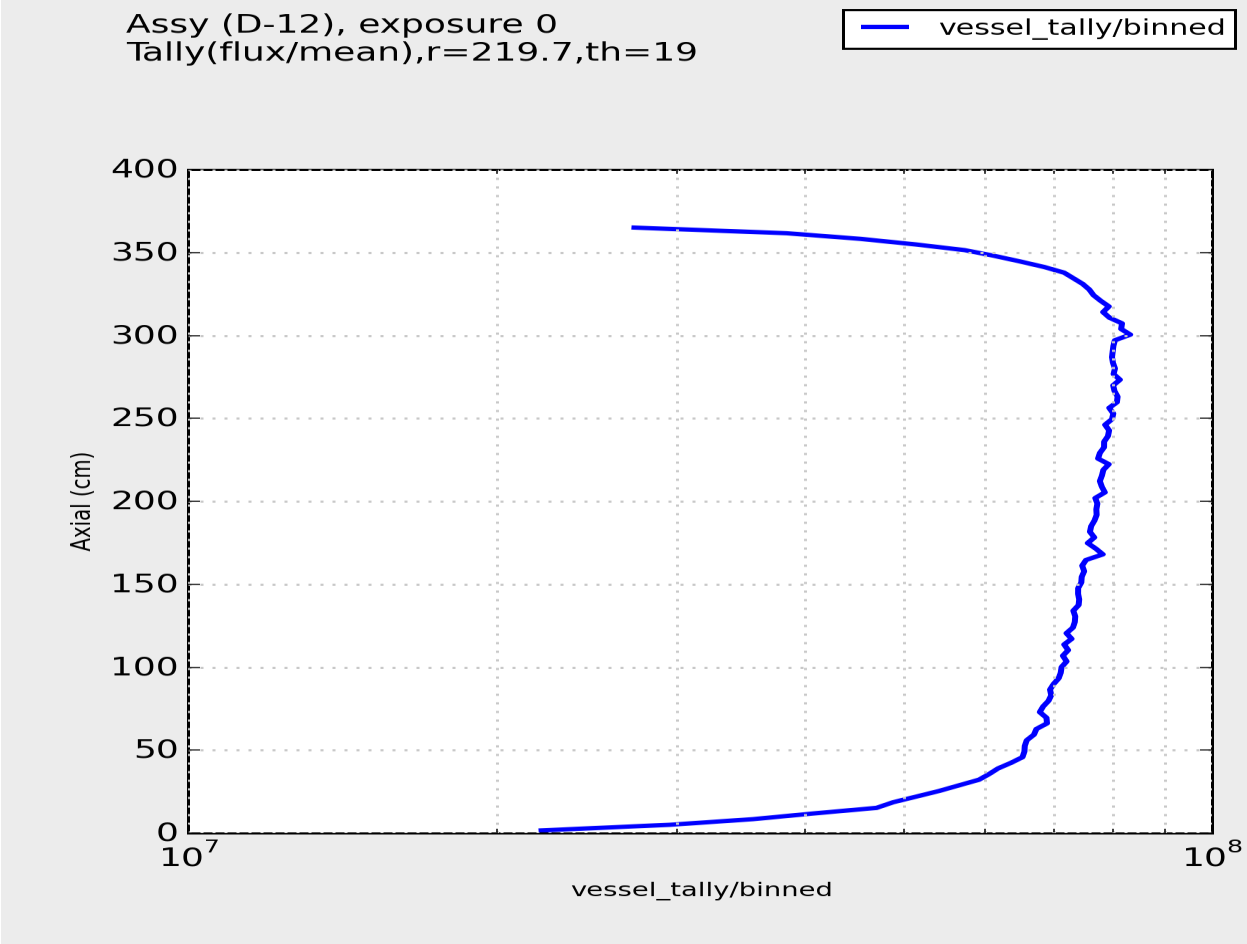
Figure 36: Plot showing the pin power axial distribution and axial fluence profile produced using VERAView for the most refined/most particles case.

4. CONCLUSIONS AND FURTHER RESEARCH

4.1 Conclusions
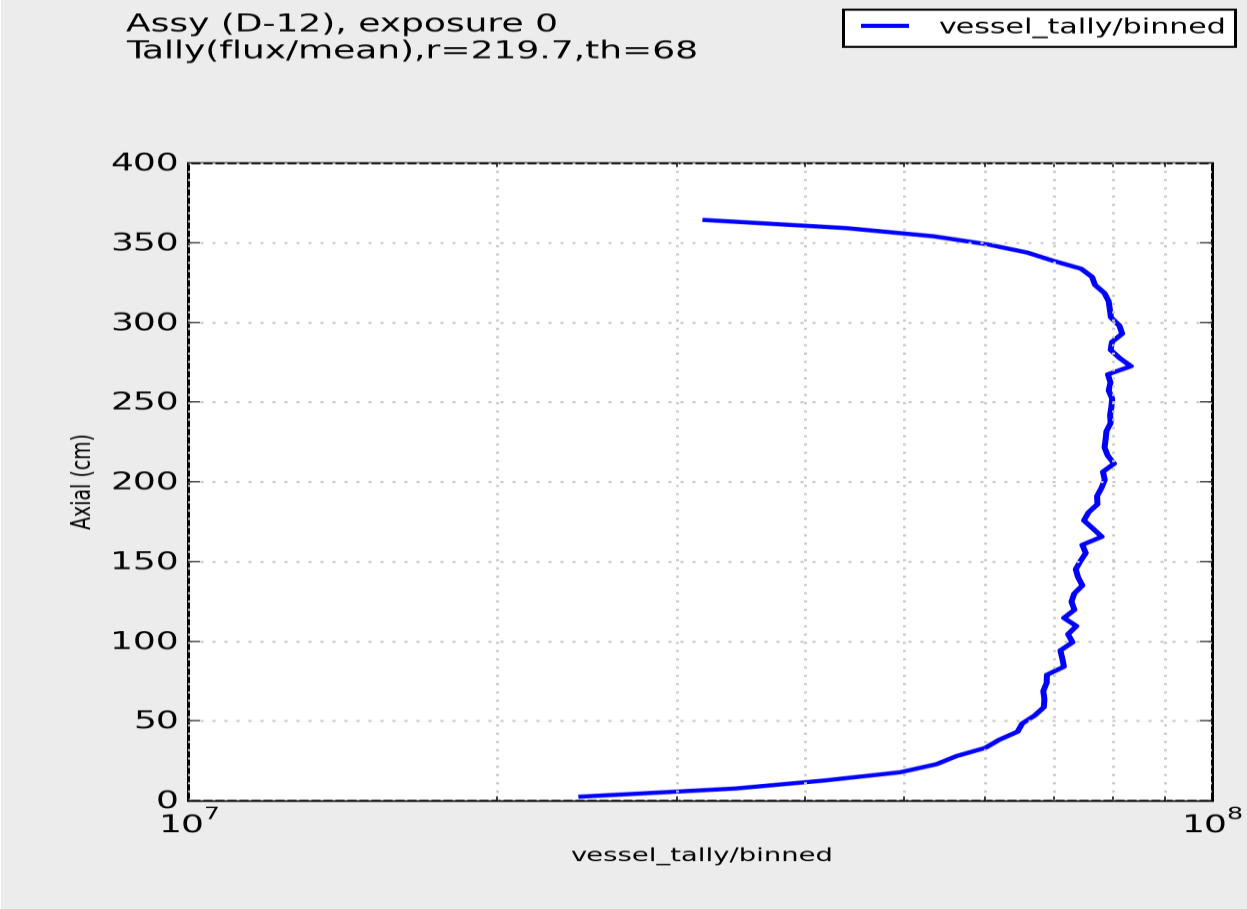
The objective of this research was to assess the current performance of the VERAShift code and to model the output behavior of the time it takes for the MC calculation to run as well as the accuracy in the reported fluence calculation. It is again noted that a primary concern for use of VERAShift in a production environment was the excessive computational resource required for industry-class machines. A performance model with predictive capability for VERAShift applicable to a production environment was the goal of this research. The developed model proved capable of predicting both time and accuracy for a variety of use-case scenarios. For a realistic operating reactor cycle depletion, a VERAShift model developed under the NRC guidelines, in terms of spatial resolution and accuracy, would require in the range of 1.8 million core-hours for 60 time state points. This is comparable to existing Monte Carlo methods that are decoupled from the core simulator. In terms of model setup complexity, VERAShift streamlines the input processing resulting in potentially many user-months of time savings, in addition to error-proofing of data transfers, from a modeling viewpoint. It is noted that the CADIS method for accelerating the VERAShift calculation was discovered to have a geometry error which limited the ability to reduce the number of particle histories with source biasing. It is expected that with a proper CADIS implementation the performance will improve significantly.

A simplified WBN1-like core was used to analyze the run time and RSD on a full core model. To do so, a design of experiments was performed to assess the importance of different factors on the output to determine those which are most influential. Once the number of inputs was reduced, a full factorial design was implemented using values based of NRC Guide 1.190. The models were found to predict the actual values closely. The predicted time slightly

overpredicts the actual time needed. The predicted RSD slightly underpredicts the actual RSD produced.

As expected, the run time increases with the number of particles used. Likewise, it was expected that the RSD would be dependent upon the tally region refinement. Both the minimum and maximum values used for refinement show similar behavior though, as the RSD decreases asymptotically with the number of particles used. When viewing the RSD versus the run time, the resulting behavior is what would be expected from a MC code. The behavior of these components of the code can be seen in **Figure 37**, **Figure 38**, and **Figure 39**.
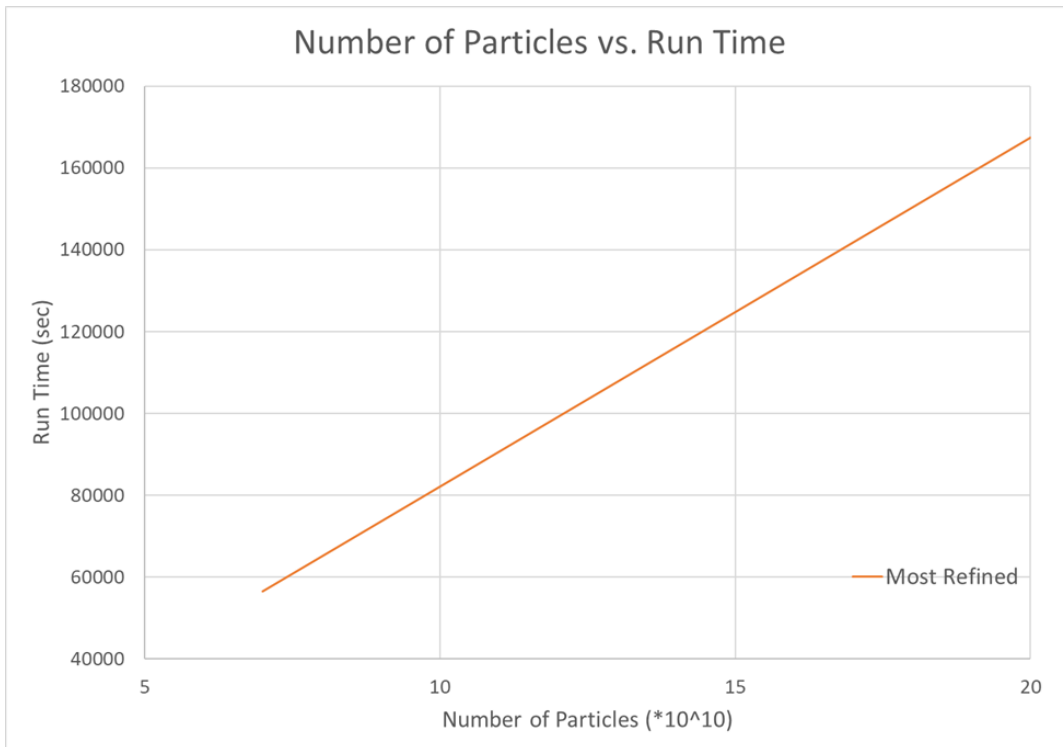
Figure 37: Behavior of the time component of the VERAShift code.
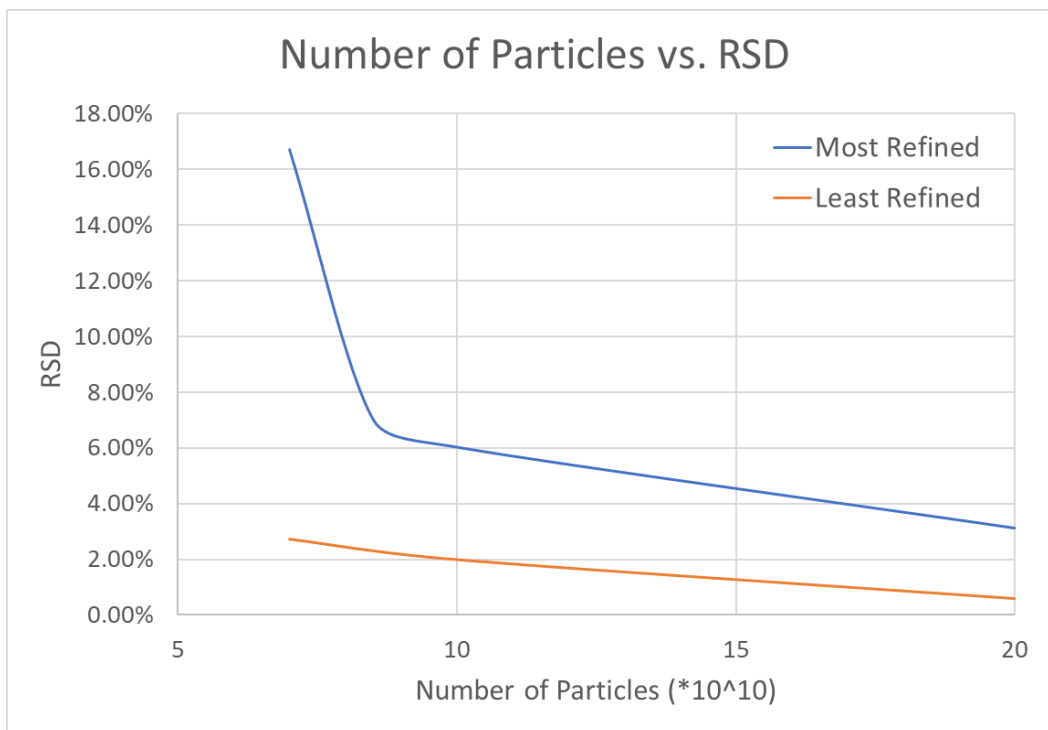
Figure 38: Behavior of the accuracy component of the VERAShift code.
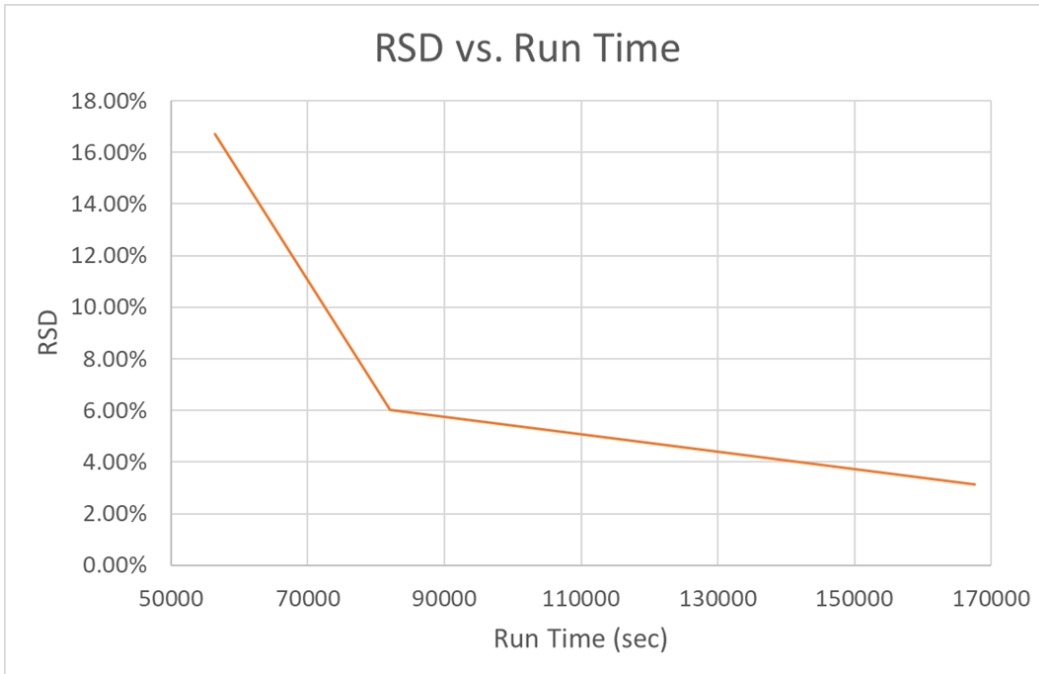
Figure 39: Behavior of the RSD versus the run time necessary to complete the execution of state point.

Current implementation of the code yields results that are promising. For the current

VERAShift and the most effective use of computational resources, 400 cores is an appropriate

number of cores to run and this is within reach of industry-class machines. While it requires a

large number of particles to achieve an RSD within limits for the NRC, the fixed version of

VERAShift with full source biasing should correct this issue. Reducing the number of particles

needed for the RSD will directly influence the total time needed for the MC calculation. By

reducing this time needed and producing a better RSD with fewer particles, VERAShift will

easily contend as a viable code for the industry.

4.2 Further Research

Though it is still under development, the results demonstrated in this report provide encouraging

evidence that VERAShift can become highly acclaimed for industrial, scientific, and educational

applications alike.

Continued development in the code will enhance the ability of VERAShift to perform excore calculations extending beyond just vessel fluence calculations, including inserting excore detectors or surveillance capsules. Another goal for VERAShift is to enable moving geometry between state points like moving control rods. Additional work on reducing memory needs is also being investigated such that full and explicit temperature and density information can be passed. This is essential to obtain full understanding of realistic core behavior.

CADIS still has some issues, including the ability to extend the mesh fully to excore features as well as mixing multigroup cross sections in excore regions. In addition to the improved CADIS implementation, the introduction of FW CADIS – a modified version of the CADIS method that scales the source at different regions of the core to account for distance – is also being worked on.

This issue, as well as working to further increase the efficiency of the code, are being resolved. Strategies for reducing the memory used, including multiple-set, overlapping domain parallelism and multithread concurrency for transport, are being explored as options for application. Continued efforts exist to further develop a more user-friendly interface and visualization tools as well for post processing results.

As it is still under development, it would be useful to perform this procedure once the updates to the capabilities of VERAShift, CADIS, and visualization tools are completed. Moving forward, it is important to continue the testing of the performance to ensure that it is properly functioning as well as producing reliable results.

REFERENCES

[1]   T. M. Pandya et al. SHIFT: A Massively Parallel Monte Carlo Radiation Transport
       Package. Technical Report CASL-U-2015-0170-000, CASL, April 19, 2015.
[2]   A. T. Godfrey. VERA Core Physics Benchmark Progression Problem Specifications.
       Technical Report CASL-U-2012-0131-004, CASL, April 29, 2014.
[3]   A. T. Godfrey et al. VERA Benchmarking Results for Watts Bar Nuclear Plant Unit 1
       Cycles 1-12. Technical Report CASL-U-2015-0206-000, CASL, June 30, 2015.
[4]   "United States Nuclear Regulatory Commission." United States Nuclear Regulatory
       Commission, United States Government, 26 Jan. 2018.
[5]   United States, Congress, Nuclear Regulatory Research. "Regulatory Guide 1.190."
       Regulatory Guide 1.190, United States NRC, 2001, pp. 1–55.
[6]   J. F. Carew et al., "PWR and BWR Pressure Vessel Fluence Calculation Benchmark
       Problems and Solutions," NUREG/CR-6115, 2001.
[7]   Fluence Calculation Methodology and Results. Technical Report 0116-20781-NP Rev. 0,
       NuScale Power LLC, December, 2016.
[8]   Wagner, J. C. and Haghighat, A. Automated Variance Reduction of Monte Carlo
       Shielding Calculations Using the Discrete Ordinates Adjoint Function. Nuclear Science
       and Engineering, 128(2):186–208, 1998.
[9]   A. T. Godfrey. Shift Testing and Benchmarking Results. Technical Report CASL-U-
       2014-0173-000, CASL, September 8, 2014.
[10]   T. M. Pandya et al. Shift Verification and Validation. Technical Report CASL-U-2016-
       1186-000, CASL, September 7, 2016.
[11]   T. M. Pandya et al. Excore Radiation Transport Modeling with VERA. Technical Report
       CASL-U-2017-1311-001, CASL, November 3, 2017.
[12]   N. C. Sly. Verification of the Shift Monte Carlo Code Using the C5G7 and CASL
       Benchmark Problems. MS thesis, University of Tennessee, Knoxville, TN, 2014.
[13]   B. Collins et al. MPACT Theory Manual, Version 2.0. Technical Report CASL-U-2015-
       0078-000, CASL, March 11, 2015
[14]   S. W. Mosher et all. ADVANTG – AN Automated Variance Reduction Parameter
       Generator. Technical Report ORNL/TM-2013/416, ORNL, November, 2013.
[15]   M. Avramova et all. Traditional MP M&S Tools and Uncertainty Treatment. United
       States NEA/NSC, 10 March, 2017.
[16]   "Design of Experiments." *Six Sigma Material,* Six Sigma. 2018.
[17]   "Fractional Factorial Design." *Wikipedia*, Wikimedia Foundation, October 7, 2017.
[18]   "Design of Experiments (DOE)." *Lean Six Sigma Training and Technology*, MoreSteam.
       2018.
[19]   Zabel, Mark. "DOE Screening and Characterizing." Online video clip, *YouTube,* May 12,
       2012.
[20]   F. G. A. Seyed and K. Hadad. Evaluation of radiation damage in belt-line region of
       VVER-1000 nuclear reactor pressure vessel. Progress in Nuclear Energy. 99. 96-102.
[21]   "Coded coefficients table for Analyze Variability." *Minitab 18 Support*, Minitab, Inc,
       2017.
[22]   "Effects Plots for Analyze Factorial Design." *Minitab 18 Support*, Minitab, Inc, 2017.
[23]   "Model summary table for Fit Regression Model." *Minitab 18 Support*, Minitab, Inc,
       2017.

[24] "Model Reduction." *Minitab 18 Support*, Minitab, Inc, 2017.

[25] "What is a Pareto chart of effects?" *Minitab 18 Support*, Minitab, Inc, 2017.

[26] "Which types of residuals are included in Minitab?" *Minitab 18 Support*, Minitab, Inc, 2017.

[27] "Methods and formulas for the model information in Analyze Factorial Design." *Minitab 18 Support*, Minitab, Inc, 2017.

[28] "Analysis of variance table for Analyze Variability." *Minitab 18 Support*, Minitab, Inc, 2017.

[29] Lund, Adam, and Mark Lund. "Linear Regression Using Minitab." *Standard Deviation | How and When to Use the Sample and Population Standard Deviation - A Measure of Spread | Laerd Statistics*, Lund Research Ltd.

[30] "Effect Size." *Wikipedia*, Wikimedia Foundation, 22 May 2018.

[31] R M. Sakia. "The Box-Cox Transformation Technique: a Review ." *The Statistician*, no. 44, 1992, pp. 169–178.

[32] T. M. Pandya et al. Verification of Vessel Fluence and Excore Modeling with VERA. Technical Report CASL-U-2018-1601-000, CASL, April 30, 2018.

[33] K. Banerjee. "Kernel Density Estimator Methods for Monte Carlo Radiation Transport." University of Michigan, 2010.

[34] J. Risner. "Multigroup Cross-Section Plotting Using the Exnihilo Python Interface." Oak Ridge National Laboratory, 5 June 2018.

[35] J. Rhodes et al. "CASMO-5 Development and Applications." Studsvik Scandpower Inc. In *PHYSOR 2006*. American Nuclear Society, September 10 – September 14.

APPENDICES

Appendix A

```
[CASEID]
  title 'CASL AMA Problem 5a-2d - Watts Bar Unit 1 Cycle 1 - Public'

[STATE]
  power    100.0
  pressure 2250            !psia
  tinlet   585 K
  tfuel    850 K
  boron    650             ! ppmB
  modden   0.7             ! g/cc
  rodbank  D 1             ! 1 = fully withdrawn
  sym      qtr
  feedback off
  xenon    equil
  search   boron
  kcrit    1.004
!  deplete  GWDMT 0.0 0.1 0.5 <1..16> 16.939


[CORE]
  size   15               ! assemblies across core
  apitch 21.5
  rated  9.3258 131.68       ! MW, Mlbs/hr
!***************************
  height 366.76
!***************************

  core_shape
    0 0 0 0 1 1 1 1 1 1 1 0 0 0 0
    0 0 1 1 1 1 1 1 1 1 1 1 1 0 0
    0 1 1 1 1 1 1 1 1 1 1 1 1 1 0
    0 1 1 1 1 1 1 1 1 1 1 1 1 1 0
    1 1 1 1 1 1 1 1 1 1 1 1 1 1 1
    1 1 1 1 1 1 1 1 1 1 1 1 1 1 1
    1 1 1 1 1 1 1 1 1 1 1 1 1 1 1
    1 1 1 1 1 1 1 1 1 1 1 1 1 1 1
    1 1 1 1 1 1 1 1 1 1 1 1 1 1 1
    1 1 1 1 1 1 1 1 1 1 1 1 1 1 1
    1 1 1 1 1 1 1 1 1 1 1 1 1 1 1
    0 1 1 1 1 1 1 1 1 1 1 1 1 1 0
    0 1 1 1 1 1 1 1 1 1 1 1 1 1 0
    0 0 1 1 1 1 1 1 1 1 1 1 1 0 0
    0 0 0 0 1 1 1 1 1 1 1 0 0 0 0

  assm_map
    1
    2 1
    1 2 1
```

```
      2 1 2 1
      1 2 1 2 2
      2 1 2 1 2 3
      1 3 1 3 3 3
      3 3 3 3

   insert_map
       -
      20  -
       - 24  -
      20  - 20  -
       - 20  - 20  -
      20  - 16  - 24 12
       - 24  - 16  -  -
      12  -  8  -

   crd_map
      A
      - -
      - - -
      - - - -
      A - - - A
      - - - - - -
      - - - - - -
      - - - -

   crd_bank
      D
      - -
      - - -
      - - - -
      D - - - D
      - - - - - -
      - - - - - -
      - - - -

   baffle ss 0.19 2.85

   vessel  mod 187.96         ! barrel IR (cm)
           ss 193.68          ! barrel OR (cm)
          mod 219.15          ! vessel liner IR (cm)
           ss 219.71          ! vessel liner OR / vessel IR (cm)
           cs 241.70          ! vessel OR (cm)

   pad ss  194.64 201.63 32 45 135 225 315 ! neutron pad ID,OD arc
lenth (degrees), and angular positions (degrees)

   xlabel  R P N M L K J H G  F  E  D  C  B  A
   ylabel  1 2 3 4 5 6 7 8 9 10 11 12 13 14 15

   bc_top reflecting
   bc_bot reflecting
```

```
[ASSEMBLY]
  title "Westinghouse 17x17"
  npin 17
  ppitch 1.26

  fuel U21 10.257 94.5 / 2.110 u-234 0.017364
  fuel U26 10.257 94.5 / 2.619 u-234 0.021947
  fuel U31 10.257 94.5 / 3.100 u-234 0.026347

  cell 1      0.4096 0.418 0.475 / U21 he zirc4
  cell 2      0.4096 0.418 0.475 / U26 he zirc4
  cell 3      0.4096 0.418 0.475 / U31 he zirc4
  cell 4             0.561 0.602 / mod    zirc4       ! guide/instrument
tube
  cell 6                   0.475 /        zirc4       ! plug

  lattice LAT21
      4
      1 1
      1 1 1
      4 1 1 4
      1 1 1 1 1
      1 1 1 1 1 4
      4 1 1 4 1 1 1
      1 1 1 1 1 1 1 1
      1 1 1 1 1 1 1 1 1

  lattice LAT26
      4
      2 2
      2 2 2
      4 2 2 4
      2 2 2 2 2
      2 2 2 2 2 4
      4 2 2 4 2 2 2
      2 2 2 2 2 2 2 2
      2 2 2 2 2 2 2 2 2

  lattice LAT31
      4
      3 3
      3 3 3
      4 3 3 4
      3 3 3 3 3
      3 3 3 3 3 4
      4 3 3 4 3 3 3
      3 3 3 3 3 3 3 3
      3 3 3 3 3 3 3 3 3

!**************************
  lattice PLUG
```

```
        4
        6 6
        6 6 6
        4 6 6 4
        6 6 6 6 6
        6 6 6 6 6 4
        4 6 6 4 6 6 6
        6 6 6 6 6 6 6 6
        6 6 6 6 6 6 6 6 6
!**************************

!**************************
  axial  1  0.0 PLUG 1.0 LAT21 366.76
  axial  2  0.0 PLUG 1.0 LAT26 366.76
  axial  3  0.0 PLUG 1.0 LAT31 366.76
!**************************

[INSERT]
  title "Pyrex"
  npin 17

  cell 1  0.214 0.231 0.241 0.427 0.437 0.484 / he ss he pyrex-vera he
ss

  rodmap  PY8
     -
     - -
     - - -
     1 - - -
     - - - - -
     - - - - - 1
     - - - - - - -
     - - - - - - - -
     - - - - - - - - -

  rodmap  PY12
     -
     - -
     - - -
     1 - - -
     - - - - -
     - - - - - -
     - - - 1 - - -
     - - - - - - - -
     - - - - - - - - -

  rodmap  PY16
     -
     - -
     - - -
     1 - - -
     - - - - -
```

```
            - - - - - 1
            - - - 1 - - -
            - - - - - - - -
            - - - - - - - -

      rodmap  PY20
            -
            - -
            - - -
            1 - - -
            - - - - -
            - - - - - 1
            1 - - 1 - - -
            - - - - - - - -
            - - - - - - - -

      rodmap  PY24
            -
            - -
            - - -
            1 - - 1
            - - - - -
            - - - - - 1
            1 - - 1 - - -
            - - - - - - - -
            - - - - - - - - -

!*************************
  axial   8  1.0  PY8   366.76
  axial  12  1.0  PY12  366.76
  axial  16  1.0  PY16  366.76
  axial  20  1.0  PY20  366.76
  axial  24  1.0  PY24  366.76
!*************************

[CONTROL]
  title "B4C with AIC tips"
  npin 17
  stroke  1.0 1

  cell 1  0.382 0.386 0.484 / aic he ss
  cell 2  0.373 0.386 0.484 / b4c he ss

  rodmap AIC
        -
        - -
        - - -
        1 - - 1
        - - - - -
        - - - - - 1
        1 - - 1 - - -
        - - - - - - - -
```

```
           - - - - - - - - -

    rodmap B4C
           -
          - -
         - - -
        2 - - 2
       - - - - -
      - - - - - 2
     2 - - 2 - - -
    - - - - - - - -
   - - - - - - - - -
!************************
  axial  A  1.0  AIC 366.76
  axial  B  1.0  B4C 366.76
!************************

[EDITS]
!************************
  axial_edit_bounds
      1
      10.37846154
      19.75692308
      29.13538462
      38.51384615
      47.89230769
      57.27076923
      66.64923077
      76.02769231
      85.40615385
      94.78461538
      104.1630769
      113.5415385
      122.92
      132.2984615
      141.6769231
      151.0553846
      160.4338462
      169.8123077
      179.1907692
      188.5692308
      197.9476923
      207.3261538
      216.7046154
      226.0830769
      235.4615385
      244.84
      254.2184615
      263.5969231
      272.9753846
      282.3538462
      291.7323077
```

```
      301.1107692
      310.4892308
      319.8676923
      329.2461538
      338.6246154
      348.0030769
      357.3815385
      366.76

!***************************

[MPACT]
  num_space        600
  par_method    EXPLICITRADIAL
  par_map          1   1   1   1   1   2   2   2   2   3   3   3   3
4   4   4   4
                   1   1   1   1   1   2   2   2   2   3   3   3   3   4
4   4   4
                   1   1   1   1   1   2   2   2   2   3   3   3   3   4
4   4   4
                   1   1   1   1   1   2   2   2   2   3   3   3   3   4
4   4   4
                   1   1   1   1   1   2   2   2   2   3   3   3   3   4
4   4   4
                   8   8   8   8   8   7   7   7   7   6   6   6   6   5
5   5   5
                   8   8   8   8   8   7   7   7   7   6   6   6   6   5
5   5   5
                   8   8   8   8   8   7   7   7   7   6   6   6   6   5
5   5   5
                   8   8   8   8   8   7   7   7   7   6   6   6   6   5
5   5   5
                   9   9   9   9   9  10  10  10  10  11  11  11  11  12
12   0   0
                   9   9   9   9   9  10  10  10  10  11  11  11  11  12
12   0   0
                   9   9   9   9   9  10  10  10  10  11  11  11  11  12
12   0   0
                   9   9   9   9   9  10  10  10  10  11  11  11  11  12
12   0   0
                  15  15  15  15  15  14  14  14  14  13  13  13  13   0
 0   0   0
                  15  15  15  15  15  14  14  14  14  13  13  13  13   0
 0   0   0
                  15  15  15  15  15  14  14  14  14   0   0   0   0   0
 0   0   0
                  15  15  15  15  15  14  14  14  14   0   0   0   0   0
 0   0   0

[SHIFT]
  problem_mode        cadis
  Np                  5000000000
```
87

```
  output_geometry true
  output_fission_source true
  transport ce
  create_unique_pins false
  transfer   fiss_src
  global_log debug
  local_log debug
! hybrid
  output_adjoint true
  Pn_order 0
  adjoint true
  eq_set sc
  mesh 1
  num_blocks_i 10
  num_blocks_j 10
  output_adjoint true
  xs_library  v7-56
  num_groups 8
  new_grp_bounds        6.0653E+06 3.6788E+06 2.3457E+06 1.6530E+06
8.2085E+05 2.4176E+04 1.0130E+02 1.0000E-05
  max_delta_z 1.0
  verbosity high
  upscatter_verbosity high
  store_fulcrum_string  false
! tally_db
  n_bounds              2.0e7 1.0e6
  num_theta             360 ! 90 per quadrant
  num_axial             80
  radial_mesh           0   187.959999 189   191   193.680001 219.149999
     219.7100001    222.4600001    225.2100001    227.9600001
     230.7100001    233.4600001    236.2100001    238.9600001
     241.70001
```